NTNU
Det skapende universitet

Process Optimization of Biogas Upgrading with AMP Using Pilot Plant Data and Simulations with Aspen Plus

Hans-Ulrik Lingelem

Industriell kjemi og bioteknologi
Innlevert: juni 2016
Hovedveileder: Hanna Knuutila, IKP

Norges teknisk-naturvitenskapelige universitet
Institutt for kjemisk prosessteknologi

Abstract

Biogas is considered as a potential source of energy to replace fossil fuels. Besides methane (CH_4), other gaseous components such as carbon dioxide (CO_2) and hydrogen sulfide (H_2S), may be generated in biogas production processes. The concentration of such components needs to be reduced to increase heating value, avoid corrosion, eliminate toxicity (H_2S, in particular) and to conform to common gas specifications, all in order to efficiently utilize the biogas. The purification process is often referred to as "upgrading". In the upgrading process, chemical absorption with amines has been identified as one of the most attractive processes. One of the major limitations of implementing amine based CO_2 removal from biogas, as for post-combustion flue gas capture pf CO_2, is the high energy loss in the process. Better process design and new solvents are developed in order to minimize the energy loss. The development of new solvents with enhanced characteristics has been an area of focus in recent times. 2-amino-2-methyl-1-propanol (AMP) is among the solvents which have shown good results in comparison to other well established solvents. The development of more efficient process design has been less studied. However, this area has also gained more attention with the increased interest in carbon capture and sequestration (CCS), and for reduced cost of implementation of CCS. Key areas of optimization for the chemical absorption process of CO_2 have been identified as: **a)** Absorption enhancement, **b)** Heat integration, and **c)** Heat pumps

In this study the implementation of a process simulation model in Aspen Plus V8.6 with AMP has been studied as a potential solvent for biogas upgrading. The simulation model is compared to experimental data for both vapor liquid equilibria (VLE) and laboratory scale pilot plant studies. It has been established that the simulation model, developed as part of this work, is well suited for simulation. For concentrations around 30[wt%] AMP in aqueous solution, and for temperatures typical for processes with CO_2 absorption using amines, 30-120 [°C]. The deviation between simulated data and experimental data from pilot tests for absorption and desorption performance, were 12.8% and 8% respectively.

It was found that the simulation model underestimated the desorption rate.

The simulation model has been used for biogas upgrading simulations with 30[wt%] AMP. Six process modifications have been applied to the conventional amine absorption process: **a)** Intercooled absorber (ICA), **b)** Rich solvent recycle (RSR), **c)** Feed gas compression (FGC), **d)** Lean vapor compression (LVC), **e)** Rich vapor compression (RVC), and **f)** Rich solvent split (RSS). From the simulations of the modifications it has been shown that significant reductions in the energy requirement of the process can be achieved. It was found that the absorption column had a large requirement for cooling in order to operate optimally. The simulation results indicated 64% reduction for the optimal solvent flow rate for ICA, and further work may demonstrate even higher reductions. LVC gave the largest decrease in reboiler duty with a reduction of 33%. The reduction in equivalent electricity (converted to equivalent thermodynamic work, i.e. how much electricity can be produced with the same amount of energy) for LVC was lower than the reboiler duty due to additional compression work, and calculated to 8.0%. RSS gave a 16% reduction in the equivalent electricity requirement.

Preface

This Master's thesis was written during the spring of 2016. It is the final part of the Chemical Engineering and Biotechnology study program at the Norwegian University of Science and Technology, leading to the degree of M.Sc in Chemical Engineering. The thesis was performed in collaboration with the Environmental Engineering and Reactor Technology group, with Associate Professor Hanna Knuutila as supervisor.

I hereby declare that this is an independent work according to the exam regulations of the Norwegian University of Science and Technology (NTNU).

Trondheim, 20th of June 2016.

Hans-Ulrik Lingelem

Acknowledgements

I would first and foremost like to express my sincere gratitude towards my supervisor Associate Professor Hanna Knuutila, for her valuable guidance and support during the work of this thesis. Her constructive attitude and encouragement has made the work with this Master's thesis a truly inspiring experience.

I would also like to thank my friends in Trondheim for five memorable years. Last but not least, I would like to tank my family for their invaluable support and encouragement.

Contents

List of Tables

List of Figures

List of Symbols

Symbol	Unit	Description
F	kmol/h	Molar flow rate
A	-	Pre-exponential factor
E_a	kJ/mol	Activation energy (kinetic model)
k	-	reaction rate constant
$N_{CO_2,abs}$	kmol/h	Absorption rate of CO_2
$N_{CO_2,des}$	kmol/h	Desorption rate of CO_2
p	bar	Pressure
Q	W	Duty
Q_R	kJ/kgCO_2	Reboiler duty
R	J/mol K	Universal gas constant
T	K	Temperature
W_{eq}	kJ/kgCO_2	Equivalent work
x	-	Mole fraction
Greek symbols		
α	-	Loading (mol CO_2/mol amine)
η	-	Efficiency
ν	-	Compared value (deviation calculation)

Abbreviations

AAD	Absolute average deviation
AD	Average deviation
AMP	2-amino-2methyl-1-propanol
CCS	Carbon capture and sequestration
CH_4	Methane
CO_2	Carbon dioxide
COP	Coefficient of performance
FGC	Feed gas compression
GHG	Green house gases
H_2O	Water
H_2S	Hydrogen sulfide
ICA	Intercooled absorber
IEA	International Enegy Agency
L/G	Liquid to gas mass flow rate
LBG	Liquid biogas
LVC	Lean vapor compression
MDEA	Methyldiethanolamine
MEA	Monoethanolamine
N_2O	Nitrous oxide
NTNU	Norwegian University of Science and Technology
OECD	Organisation for Economic Co-operation and Development
PSA	Pressure swing adsorption
Pz	Piperazine
RSR	Rich solvent recycle
RSS	Rich solvent splitting
RVC	Rich vapor compression
VLE	Vapor liquid equilibrium

Chapter 1

Introduction

1.1 Objective

Biogas is a growing energy source. Leading countries like Germany and Sweden have committed to replace increasingly more fossil fuel with renewable biogas. In order to meet the required specifications for the biogas, upgrading is necessary, i.e. removal of components like carbon dioxide (CO_2) and hydrogen sulfide (H_2S) which may be formed along with methane (CH_4) when generating biogas. Chemical absorption has proven to be one of the most promising technologies for this purpose. In order to improve upgrading processes both pilot plants and simulation software are important tools. Pilot testing is important for obtaining reliable data on the kinetics of absorption and energy usage, both as an empiric basis by itself and as a basis for simulations. The results from pilot plants also used used as basis for and to validate the results from the process simulation.

Simulation software is used to extend the analysis of a plant beyond that of experiments. This includes extensions to full scale plants. The accuracy of the process simulation is important for arriving at reliable results on which the design of chemical plants are based. Simulation tools are an important element in testing how new solvents will perform in full scale processes. Good and reliable process simulators can greatly reduce the cost of development of new plants and to prepare for their operation, by establishing operation conditions, equipment sizing and optimization.

The first objective of this thesis is to establish a simulation model for CO_2-absorption with hydrous 2-amino-2methyl-1-propanol (AMP), using Aspen Plus version 8.6. The basis for developing the simulation model is a template provided as a part of the software. The model has been extensively compared to experimental data for the fluids and available pilot data.
The second objective is to use the model to test possible process designs suggested for biogas upgrading. This include testing how well AMP performs in biogas upgrading, and how process modifications can reduce the energy demand of specific processes.
The third objective is to optimize the most suitable designs identified in the second objective. With the ambition to further increase the efficiency of this setup.

1.2 Outline of Thesis

The background for studying biogas upgrading is given in Chapter 1. The current status of biogas upgrading internationally, and in Norway are also discussed in this chapter. Chapter 2 includes the necessary background information, such as a general process descriptions, and more information about the solvent and the reactions occurring in the system. Chapter 3 deals with relevant literature, including CO_2 capture using AMP and typical process modifications regarding chemical absorption. Chapter 4 explains the simulation model established in Aspen Plus, based upon the available template. The procedure for evaluating the model is established in this chapter. Chapter 5 compares simulated data and experimental data form a pilot plant. Chapter 6 presents the input structure of the base case and process modifications. Chapter 7 presents the simulation results of the base case and the process modifications. Chapter 8 presents the conclusion og suggested further work.

1.3 Motivation

1.3.1 Reduced Energy Consumption and Reduction of Emission of Green House Gases

In recent times the earth's atmosphere has experienced increased levels of gases which may be traced back to anthropogenic sources, such as production and burning of fossil fuels. Several of these gases trap some of the energy from the sun in Earth's atmosphere, by absorbing an re-emitting thermal radiation from Earth. Because of this effect they are commonly known as greenhouse gases (GHG). Among the most common ones are CO_2, CH_4, nitrous oxide (N_2O) and fluorinated gases (Water vapor is also important, but mainly not due to anthropogenic emissions). Since the industrial revolution the emission of anthropogenic GHGs has increased significantly. As a result it is commonly argued that the Earth will

experience a further rise in temperature in the future with associated changes in the global environments and weather systems. Assuming that present simulations of the Earth climate remain correct, it will be necessary to drastically reduce the emissions of the GHGs to limit the increase of Earth's temperatures. Earth's population is growing and at the same time the energy consumption per capita is increasing. Developing countries are increasing their standard of living and with an associate increase of the use of energy, largely as an increase of fossil hydrocarbon fuels. As a result the worlds energy demand is expected to increase and the emission of GHGs with it. In order to limit the net emission of GHGs it will be necessary to both increase efficiency of the use of fuels, use more sustainable fuels and possibly capture and sequesting of GHGs as a part of the processes for energy production.

Perspectives on the past

The increased acknowledgement of a potential global warming and climate change has lead to an intensification of research on sustainable energy resources and reducing the emission from conventional fossil fuels. The concentration of CO_2 in the atmosphere has increased at a growing pace since the industrial revolution and is still increasing at a fast pace. Figure 1.1 shows measurements of the atmospheric concentration of CO_2, from probably the most comprehensible recordings, performed at Mauna Loa Observatory in Hawaii. A study by [1] made measurements on the CO_2 and CH_4 content of the ice core of Eastern Antarctica, enabling measurements of composition of air pockets from a more distant past. This study reported that "Atmospheric concentrations of carbon dioxide and methane correlate well with Antarctic air-temperature throughout the record. Present-day atmospheric burdens of these two important greenhouse gases seem to have been unprecedented during the past 420,000 years".

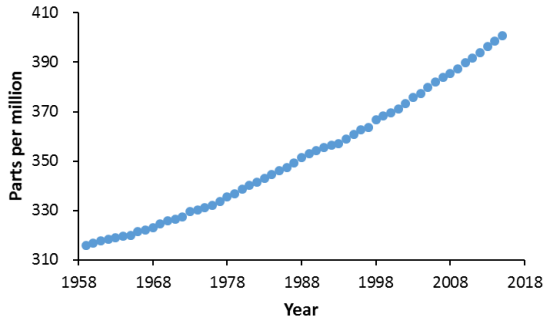

Figure 1.1: Figure showing the measured CO_2 concentration in the atmosphere at Mauna Loa Observatory in Hawaii[2]

.

Outlook to the future

The energy company BP's forecast for 2035 has estimated that the energy consumption will continue to grow towards 2035. Fossil fuels will remain the main source of energy, with a share of 80% [3]. Further they estimate a rise in consumption of both natural gas and biofuels, with an increase from 3-9% for all renewables including biofuels. Estimates for CO_2 emission show a growth in yearly emissions of 20% between 2014 and 2035. Figures of BP's estimates can be seen in Figure 1.2. They identify a major role for CO_2 capture in combating growing emissions. The International Energy Agency (IEA) has presented similar high estimates for growth in energy demand as well as growth in gas consumption, and CO_2 emissions [4].

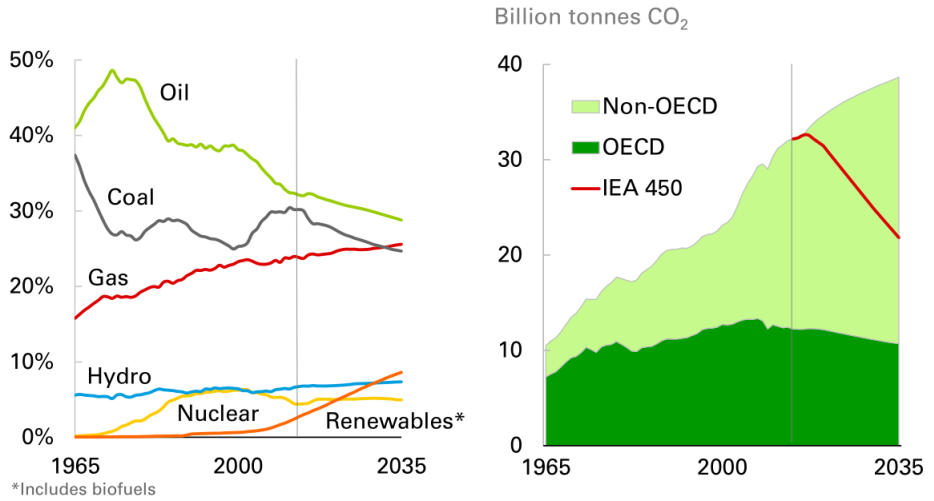

Figure 1.2: Figures showing estimates of the total energy consumption as percentages of each major resource to the (left) and the global CO_2 emission (right)[3]. The IEA 450 line is showing the scenario "IEA 450" stated by IEA, where there is a 50% chance of limiting the global warming to 2 [°C] in the long term

.

The total global anthropogenic green house gas emission can be broken down by economic sectors [5],

- Transport: 14%
  - Fossil fuels to run vehicles, ships, planes etc.
- Industry: 21%
  - Carbon intensive manufacturing processes such as steel, cement and petrochemical production.
- Electricity and heat production: 25%
  - Electricity production by fossil fuels.
- Agriculture, forestry and other use of land: 24%
  - Deforestation is a major contributor to carbon dioxide emissions, at the same time as the global CO_2 uptake is reduced if forests are not replanted.

In order to reduce the net amount of CO_2 released into the atmosphere efficient and cost effective processes need to be developed and implemented in the energy industry, possibly including CO_2 capture and sequestering(CCS), and sustainable fuels and other renewable energy sources need to enter the market. [6] has defined CCS as a set of technologies that can greatly reduce the CO_2 emissions from new and existing coal- and gas-fired power plants and large industrial sources. CCS is a three-step process that includes:

- Capture of CO_2 from power plants or industrial processes
- Transport of captured and compressed CO_2 (usually in pipelines)
- Underground injection and geologic sequestration (also referred to as storage) of the CO_2 into deep underground rock formations. These formations are often a mile or more beneath the surface and consist of porous rock that holds the CO_2. Overlying these formations are impermeable, non-porous layers of rock that trap the CO_2 and prevent it from migrating upward.

1.3.2 Biogas

Biomass-derived fuels and energy products have been suggested as a part of the change from fossil fuels to renewable and sustainable sources. Biogas can provide an alternative to complement to-, and ultimately a replacement for fossil fuels. Biogas can be produced from a variety of feedstocks on a large portion of the globe. Biogas has a potential for lower environmental impact compared to fossil fuels and even carbon negativity if combined with with CCS. A major advantage of biogas is that upon upgrading to biomethane it can be distrubuted and consumed along with, or mixed with, fossil natural gas. Hence making use of already installed infrastructure and consumer systems.

Biogas is derived from biomass. This includes all plant and plant-derived materials, animal manure, and waste from food production. Not only, as many may believe, sugar, starch and other high energy/value crops, possibly in competition with food production. The basis for biomass can be a wide variety of forestry and agricultural resources and by-products, industrial-process residues, and municipal-waste.

1.3.3 Biogas Upgrading

Biogas production is growing and there is an increasing demand for upgraded biogas, to be used as vehicle fuel or injected in to a natural gas grid. Figure 1.3(b) displays the increase in production of upgrading plants. Efficient use of the biogas and adherence to common product specifications require the biogas to be upgraded, i.e. separating impurities such as CO_2 and H_2S from methane. The United Kingdom, Sweden and Germany have been at the forefront for developing and implementing biogas upgrading plants. This can be seen in Figure 1.3(a). For the Norwegian market, the growth has been modest, possibly due to the large reserves of natural gas and relatively low use of natural gas. However, the potential has been acknowledged and biogas plants have been built and being planned.

The main motivations for upgrading of biogas are stated below,

- Presence of CO_2 reduces the heating value of the gas an may cause problems with gas combustion equipment.
- Presence of water reduces the heating value of gas. It may also form gas hydrates and cause corrosion.
- H_2S is a poisonous gas and is highly corrosive. In order to reduce the wear on process equipment and piping, and for safety reasons, it should be removed as early as possible.
- CO_2 is a potent greenhouse gas and should be removed and stored to prevent it from entering the atmosphere.

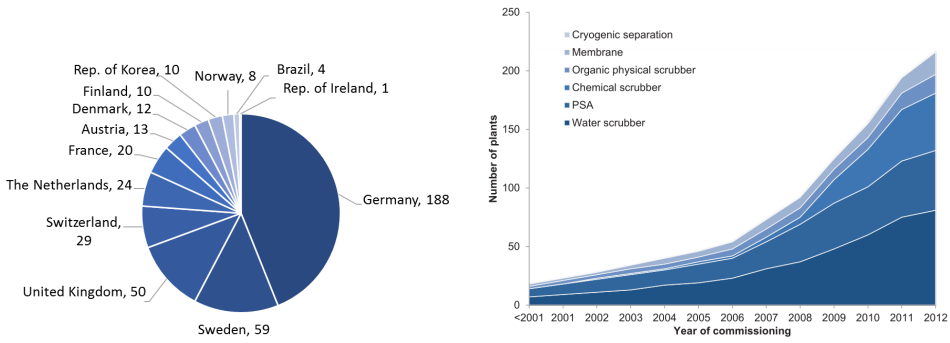

Figure 1.3: Figure a) showing the distribution for 2015 of biogas upgrading units per country [7]. Figure b) gives a visualisation of yearly number of manufactured biogas upgrading plants, and the technology applied in these plants [8].

Since biogas is derived form several sources and has a variety of compositions several methods may be considered for upgrading the gas, taking into consideration the concentration and combination of the different elements to be removed. Some of the most commonly used are and commercial available are; **a)** Amine scrubbing **b)** Pressure swing adsorption **c)** Membrane separation **d)** Water scrubbing and **e)** Organic physical scrubbing.

The decision of the method to use is mostly influenced by the desired characteristics of the upgraded gas, and also by the required robustness and complexity of the process.

1.3.4 Biogas Upgrading in Norway

For the Nordic countries such as Norway and Sweden, production of biofuels from high energy crops is not considered viable, mainly due to alternative uses of and as food, in particular. As an alternative, biogas can be produced from several resources which are already available, but not developed. A biogas production and upgrading plant in Skogn, Nord-Trøndelag, built for Norske Skog, will be the largest production plant for liquid biogas (LBG) in the Nordic countries. The planned production capacity is 25 million [Nm^3] [9], the equivalent CO_2 emission of some 25,000 diesel automobiles. This plant alone will double the Norwegian biogas production, and has received financial support from the Norwegian government through ENOVA, showing that biogas is a priority area. The plant utilizes biomass waste from forestry and fish industries. Expertise from the oil and gas

industry has been used for the design of the plant. A biproduct of the process is climate friendly fertilizer which can be distributed to farmlands in the area around the site. Other large biogas plants in Norway are found in the densely populated areas in Tønsberg [10] and Romeriket [11]. Here food wastes are used for the biogas production. The produced biogas is mainly used in the public transport sector. For 2016, Innovation Norway (the Norwegian Government's most important instrument for innovation and development of Norwegian enterprises and industry), has put up 20 million [NOK] for pilot testing of biogas production in Norway [12].

Chapter 2

CO_2 Absorption Using AMP as a Solvent

2.1 General Process Description

This chapter gives a generic overview of a typical amine absorption process. Many different layouts of the process exists, but the basics are similar based upon the patent by [13] from 1930. The general process for chemical absorption of CO_2 using amines are principally made up of an absorption column and a stripper. The process was greatly improved during the oil crisis between 1973 and 1980, and has recently gained a lot of attention with the focus on CCS. The process allows the amine to be recycled in the process, separating CO_2 from the gas stream and releasing CO_2 in the stripper. The amine scrubbing process is a thermal swing process in which the different equilibrium amounts of CO_2 in the amine/water solution at different temperatures is used to absorb and desorb CO_2. The thermodynamics of the amine absorption/desorption reactions are such that absorption is a exothermic reaction and desorption/stripping is a endothermic reaction.

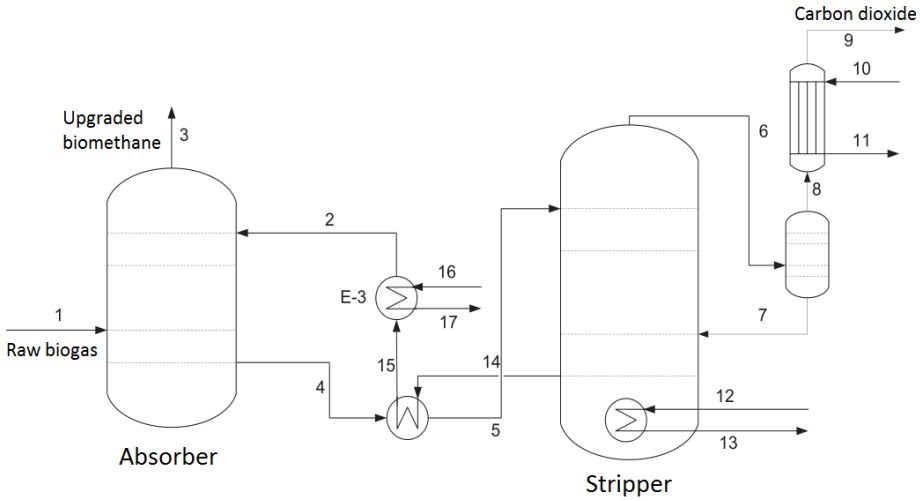

Figure 2.1: A generic process flow diagram of chemical removal of CO_2 using amines

.

The basic principle of the amine process is given in Figure 2.1. The inlet gas stream (1) enters in the bottom of the absorption column. The gas is contacted with the lean amine (2) in the absorption column. The acid gases reacts with the amine and transferred out with the rich amine stream (4). Upgraded gas leaves the column at the top of the column (3). The absorption reaction is exothermic and raises the temperature in the column, typically from 20-40 [°C] to 45-65 [°C]. The operating pressure of the absorber is typically in the range 1-2 [bar(a)].

The rich amine (4) is then preheated using the hot exit stream from the stripper (14). The heated rich amine (5) is then routed to the top of the stripper column. In the stripper column the rich amine is further heated to release CO_2. The reboiler (12-13) in the bottom of the stripper column provides heat at 120-150 [°C] typically with steam or hot water/oil. The function of the reboiler is twofold; it increases the temperature to release CO_2. It also creates free water vapor which lowers the partial pressure of CO_2 to further increase the release from the rich amine. The pressure in the stripper is slightly higher than the absorber, typically 1.5-3 [bar(a)].

The acid gases exit in the top of the stripper (6). The stream is then cooled in a condenser in order to collect water vapor and carry over amine. This is then returned to the stripper (7). For biogas production there is typically a gas sweetening unit (H_2S removal) unit up stream of the CO_2 removal unit.

2.2 2-amino-2-methyl-1-propanol(AMP)

A good solvent is generally characterized by the following properties [14, 15]:

1. High selectivity for CO_2
2. High stability (Volatility, degradation, corrosion etc.)
3. High maximum solvent loading
4. Low lifetime cost
5. Wide envelope of possible operating conditions, such as pressure, temperature etc.
6. Low enthalpy of absorption. Often directly linked to the energy penalty of the scrubber system.

An intrinsic challenge associated with the use of alkanolamines as absorbents for CO_2 is the required energy for regeneration of the CO_2-rich solvent. Conventional alkanolamines can be classified into three chemical categories: primary, secondary and tertiary amines. The primary amines such as Monoethanolamine (MEA) shown in Figure 2.2(a) is considered the most suitable for flue gas cleaning because of the low partial pressure of CO_2 in the flue gas. MEA is one of the most industrially important alkanolamines, attractive at low partial pressures of CO_2. MEA reacts rapidly and the cost of raw solvent is low compared to more complex amines. However, MEA has high regeneration energy, low loadings (up to 0.5 mol CO_2/ mol MEA), and problems regarding corrosion, solvent loss and solvent degradation [16]. Tertiary alkanolamines such as Methyldietanolamine (MDEA), can reach higher loadings (up to 1 mol CO_2/mol MDEA) and has reduced energy of regeneration. The low rates of reaction makes tertiary amines less suitable for flue gas cleaning. However, at the moment Methyldietanolamine (MDEA) activated with Piperazine (Pz) is the amine mostly used for chemical biogas upgrading[7]. Were MDEA has high loading capacity and Pz has fast kinetics.

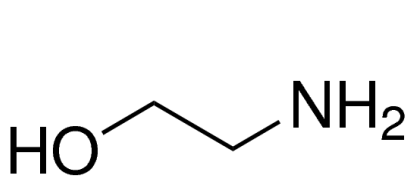

(a) MEA molecule structure

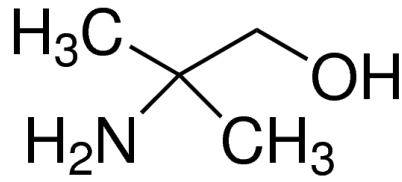

(b) AMP molecule structure

Sterically hindered amine such as AMP were presented by [17]. The molecular structure of AMP is shown in Figure 2.2(b). AMP is a hindered primary alkano-

lamine, and can be viewed as the hindered form of MEA [18]. AMP is deemed one of the most important sterically hindered amines for natural gas treatment processes [19]. Sterically hindered amines have a bulky structure. This inhibits the formation of stable carbamate ions. This might be beneficial for regeneration cycles, because it enhances the effectiveness of the process [20]. The advantageous properties of AMP are; low carbamate stability thus high loading capacity up to 1 mol CO_2/ mol AMP, much higher reaction rates compared to MDEA[19], easy regeneration at low temperature[21, 22] and resilience to degradation[23]. Sterically hindered amines can be a suitable choice for both flue gas cleaning and higher CO_2 concentration cleaning such as biogas upgrading. A less favourable property of AMP is that it has been found to have higher volatility than for other commercially available amines, such as MDEA [24, 25]. As a result higher amine losses can be expected for AMP.

2.3 Chemical Reactions

The absorption process of CO_2 and H_2S into AMP is called chemisorption. The absorption process involves the gases being chemically bound to the amine. The chemical reactions involved with the capture of CO_2 and H_2S are represented by a template available in Aspen Plus, given in the Table 2.1. The reaction products in the AMP/CO_2/H_2O system are predominately the bicarbonate species.

Table 2.1: Chemical reactions determined in the template provided in Aspen Plus

Reaction Number	Reaction Type	Stoichiometry
1	Equilibrium	$2H_2O \longleftrightarrow H_3O^+ + OH^-$
2	Equilibrium	$HCO_3^- + H_2O \longleftrightarrow CO_3^{2-} + H_3O^+$
3	Equilibrium	$AMPH^+ + H_2O \longleftrightarrow AMP + H_3O^+$
4	Equilibrium	$H_2S + H_2O \longleftrightarrow HS^- + H_3O^+$
5	Equilibrium	$HS^- + H_2O \longleftrightarrow S^{2-} + H_3O^+$
6	Kinetic	$CO_2 + OH^- \longrightarrow HCO_3^-$
7	Kinetic	$HCO_3^- \longrightarrow CO_2 + OH^-$
8	Kinetic	$AMP + CO_2 + H_2O \longrightarrow AMPCOO^- + H_3O^+$
9	Kinetic	$AMPCOO^- + H_3O^+ \longrightarrow AMP + CO_2 + H_2O$

The standard water dissociation is given in Reaction 1. Reaction 2 gives the second dissociation step of CO_2. Reaction 3 gives the protonation step of the amine. Reaction 4 and 5 gives the first and second protonation step of H_2S respectively. Reaction 6 represents the first protonation step of CO_2. Reaction 7 states the opposite of reaction 6. Reaction 8 represents the reaction between AMP and CO_2 forming carbamate($AMPCOO^-$). Reaction 9 represent the reversion of carbamate

formation. The reactions with H_2S are included here because of their possible relevance with the AMP system, although H_2S is not evaluated in this project.

The absorption of CO_2 onto AMP is exothermic. Also, the ability of AMP to absorb CO_2 is reduced with increasing temperature. Therefore temperature control is desirable in the absorption column to limit the temperature increase. However, there is a trade-off between favourable reaction/absorption temperatures, and the diffusion rates, which increases with temperature. The temperature is therefore not as low as possible for a cost effective absorption column. For the stripper, the reaction is endothermic, hence higher temperatures are needed to desorb the CO_2 from the amine. In the stripper there is also a trade-off between effective stripping, and solvent loss due to evaporation and degradation. The different thermodynamics of the reactions in the absorption and stripper column, give a variable absorption/desorption profile along the column. [26] has given the heat of absorption for different amines.

Compared to MDEA, the heat of absorption at 40 [°C] has been found to be much higher for AMP than for MDEA. One could therefore expect higher temperatures in the absorption column, compared to MDEA systems. The heat of absorption for loadings in the range 0-0.5 is around 90-80 [kJ/molCO_2] for AMP and around 60-50 [kJ/molCO_2] for MDEA [26]. At 120 [°C], MDEA was found to have lower absorption capacity than AMP, indicating more regeneration energy is required in the stipper column when AMP is used. However, MDEA was also has a lower reaction rate than AMP.

Chapter 3

Literature Review

3.1 Other Industrially Relevant Upgrading Techniques

Upgrading Technologies

There are mainly the four commercially available upgrading technologies in addition to amine scrubbing (Described in Section 2.1). These are water scrubbing, pressure swing adsorption (PSA), membrane separation and physical scrubbing with organic solvents. Cryogenic upgrading is a technology under development and demonstration, it is not considered a mature technology and not considered in this study.

3.1.1 Water Scrubbing

Water scrubbing is the most common technique in Sweden for removal of CO_2 from biogas [7]. A water scrubber is a physical scrubber which utilizes the difference in solubility in water for CH_4 and CO_2. CO_2 which has a much higher solubility is absorbed by the water and hence separated from the raw biogas. Other impurities such as hydrogen sulphide and ammonium are also physically dissolved in water. In order to achieve a good separation and to increase the driving force of solubility, a relative high pressure is used in the column. Typically operating at pressures around 6-10 [bar(a)] [7]. A process flow diagram for a typical and simplified process is shown in Figure 3.1.

Condensed water is first removed from the raw biogas before the gas is compressed and fed to the bottom of the absorption column. The gas meets a counter current water flow fed from the top of the column. The column is typically filled with a packing material in order to maximize the mass transfer. The CO_2 in the raw biogas

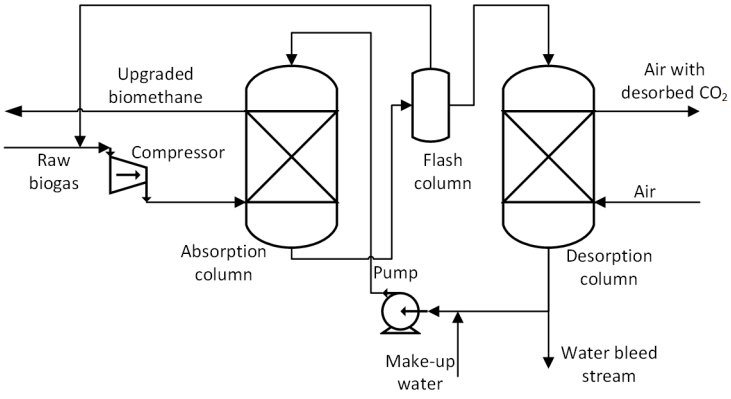

Figure 3.1: A process flow diagram for basic water scrubbing, based on [7]

.

is absorbed by the water, and an upgraded gas stream with high methane concentration leaves the top of the column. The rich water is sent to a flash tank where the pressure is abruptly reduced to pressures around 2.5-3.5 [bar(a)], the flashed gas stream is fed to the raw biogas inlet stream before the compressor. This is aimed to cut methane losses. The remaining CO_2 is released from the water in the desorption column, by addition of counter current air flow at atmospheric pressure. The desorption column is design much like the absorption column, with a packing material to maximize mass transfer. The regenerated water is in most modern cases pumped back to the absorption column in order to reduce water usage. However, the recirculation of water increases the energy use due to purification and pumping of the water.

3.1.2 Organic physical absorption

Organic physical absorption is similar to water scrubbing. The difference being that organic solvents are applied as scrubbing liquid, such as Gensorb, Selexol, Sepasolv, Rektisol and Purisol. The advantage of applying these solvent is the increased solubility of CO_2, compared to that of water, and more environmental friendly compared to amines. This results in reduced solvent flow rates, hence smaller equipment sizes are needed for the same gas rate capacity. Heating is needed before the solvent is fed to the desorption column, then cooled before entering the absorption column. CO_2 has 17 times higher solubility in the Gensorb, the most common of the organic solvents consisting of polyethylene glycol dialkyl ethers, than in water [7].

3.1.3 Pressure Swing Adsorption

This technique separates different substances on the basis of physical forces and molecular size, which dictates the penetration ability in a material. The driving force of the separation is pressure differences, where CO_2 is absorbed at high pressures and desorbed at low pressures. The alteration between high and low pressure leads to an effective absorption/desorption process. A major advantage of the process is the dry separation without the use of a solvent, hence no additional water is added in the process.

Raw biogas is compressed to elevated pressures and fed to an absorption column witch retains the CO_2 but not the methane. When the material in the column is saturated the pressure is released and CO_2 is removed from the system. For continuous operation a train of columns are needed in order to open and close consequently. The characteristics of the PSA are the feed pressure, purging pressure, absorbent properties, cycle time and column interconnectedness. A processes flow diagram of a basic and simplified pressure swing asdsorption process can be viewed in Figure 3.2.

The pressure release is typically performed in several stages. The gaseous stream initially drawn is typically sent back to the raw biogas stream in order to decrease methane loss. The absorption materials are often made of molecular sieves (zeolites), typically activated carbon. The materials used are sensitive to H_2S and water which may cause irreversible degradation. As a result these compounds normally have to be removed pre entering the absorption column.

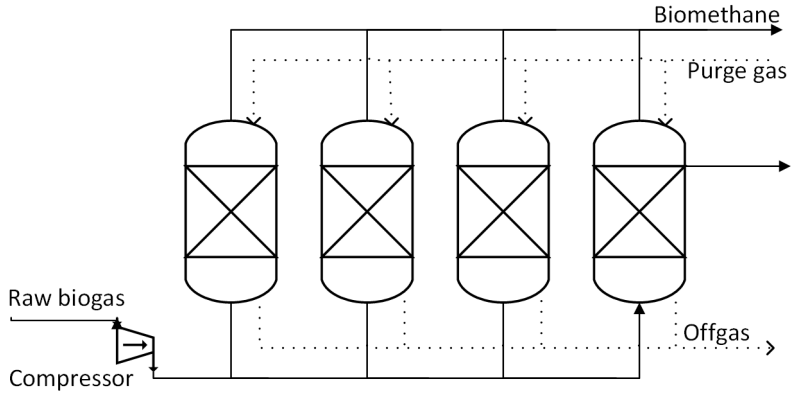

Figure 3.2: A process flow diagram for basic pressure swing adsorption, from [7]

.

3.1.4 Membrane Technology

Membranes for biogas upgrading are made of materials with low permeability for methane and high permeability for compounds to be separated. Very little methane normally permeate through the membrane. The membrane is a physical barrier through which most of the easy permeable compounds are separate from the less permeable. Hollow fibres are often the most applied configuration in order to achieve a high surface area for separation.

The raw biogas is compressed to the applied operating pressure typically around 6-20 [bar(a)], then cooled down for drying. After reheating with compressor waste heat the remaining H_2S is removed by means of adsorption on iron or zinc oxide. The gas is then piped to the membrane units, which is arranged as a single or multi-staged unit. The methane recovery level and specific compression energy demand are often set as the determining factors of the process, and not the desired biomethane quality. A process flow diagram for a basic and simplified membrane technology process is shown in Figure 3.3.

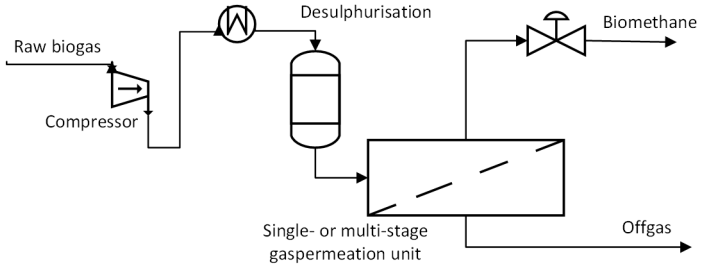

Figure 3.3: A process flow diagram for basic membrane technology process

.

3.1.5 Comparison of Upgrading Methods

These common biogas upgrading technologies are all feasible. The scrubbing technologies all perform well and have similar costs of investment and operation. Water scrubbers are relatively simple and have high reliability, which makes it the most popular method. Amine scrubbers have the advantage of high purity and low methane slip. For membranes and PSA units the investment cost is about the same as for the scrubbers. Recent developments in membranes makes it possible to reach higher purities of methane. Due to differences in local conditions, requirements as well as cost and availability of energy, it is often difficult to establish a universal valid comparison of available technologies. Table 3.1 shows a summary of the reviewed technologies and the most important parameters.

Table 3.1: A technical overview of the five commercially available technologies for biogas upgrading[7]

Parameter	Water scrubbing	Organic physical scrubbing	Amine scrubbing	PSA	Membrane technology
Typical methane content in biomethane[vol%]	95.0-99.0	95.0-99.0	>99	95.0-99.0	95.0-99.0
Methane recovery[%]	98	96	99.96	98	80-99.5
Methane slip[%]	2	4	0.04	2	0.5-20
Typical delivery pressure [bar(a)]	4-8	4-8	0	4-7	4-7
Electric demand [kWh/m3 biomethane]	0.46	0.49-0.67	0.27	0.46	0.25-0.43
Heating demand and temperature level	-	medium 70-80°C	high 120-160°C	-	-
Desulphurisation requirements	process dependent	yes	yes	yes	yes
Consumables demand	antifouling agent drying agent	organic solvent non-hazardous	amine solution hazardous, corrosive	activated carbon non-hazardous	
Partial load range[%]	50-100	50-100	50-100	85-115	50-100
# of reference plants	high	low	medium	high	low
Typical investment costs [€/(m3/h) biomethane]					
100m3/h	10,100	9,500	9,500	10,400	7,300-7,600
250m3/h	5,500	5,000	5,000	5,400	4,700-4,900
500m3/h	3,500	3,500	3,500	3,700	3,500-3,700
Typical operational costs [€/(m3/h) biomethane]					
100m3/h	14.0	14.8	14.4	12.8	10.8-15.8
250m3/h	10.3	10.2	12.0	10.1	7.7-11.6
500m3/h	9.1	9	11.2	9.2	6.5-10.1

As can be seen from Table 3.1 amine scrubbing has the lowest electricity requirement, along with the most modest values for membrane separation. The heat consumption in the stripper column, accounts for a large portion of additional required energy. Typical values given from amine upgrading plants are given in Table 3.2, given from different amine upgrading plant vendors.

Table 3.2: Amine upgrading plant consumables [7]

Electricity required	[kWh/Nm3]	0.14
Heat required	[kWh/Nm3]	0.55
Methane slip	[%]	0.06
Chemicals carry-over[a]	[kg/Nm3]	3.0E-05

[a] Including anti-foam, amine make-up, etc.

3.2 Process Modifications

One of the major challenges to optimal implementations of amine based chemical absorption of CO_2 is the energy demand in the process and considerable energy loss. The energy for 90% CO_2 capture is equivalent to 2% loss of the methane product from natural gas purification [28] . Limiting this loss can be achieved by designing new solvents and/or optimizing the process design, integration with sources of heat such as power plants or biogas production. While new solvents have been extensively studied since around year 2000, less work has been carried out for improving the process design or process integration. The related literature on this topic is quite limited. Hence the improved understanding on this topic can prove to be an important source for reducing energy needed in the process(es). Most of the studies published [23, 27, 28, 29, 30, 31] on improved process design are mainly focused on specific process modifications. In regards to chemical absorption in biogas upgrading, another limitation of the published material is the focus on CO_2 capture from high flow rate, low pressure flue gases from combustion, with the application of well used and relatively cheap MEA. A recent study by [32] made efforts of a systematic approach for evaluation of process modifications available in the open literature including patented modifications. Their findings evaluated a number of studied modifications and categorized each of them. The authors identified three areas of relevant process modifications; 1) Absorption enhancement, 2) Heat integration, and 3) Heat pumps.

3.3 Studied Process Modifications

Various process modifications have been evaluated against a base case which is the conventional chemical absorption process explained in Section 2.1. In the findings by [33] the authors addressed the importance of capital cost, operational cost and plant complexity in regards to potential process modifications. Based on the literature survey [23, 27, 28, 29, 30, 31, 32, 33, 34], processes which are low in additional complexity and additional equipment where selected for further analysis. The modifications considered in the present study are stated below:

- Absorption enhancement
  - **Intercooled absorber (ICA)**
  - **Rich solvent recycle (RSR)**
  - **Feed/flue gas compression (FGC)**
- Heat integration
  - **Rich solvent splitting (RSS)**
- Heat pumps
  - **Lean vapor compression (LVC)**
  - **Rich vapor compression (RVC)**

3.3.1 Base Case

The conventional absorber/stripper design for chemical absorption explained in Section 2.1 is shown in Figure 3.4 for comparison with the modifications explained. Modifications to the base case are shown in blue on the process flow diagrams included in the following sections.

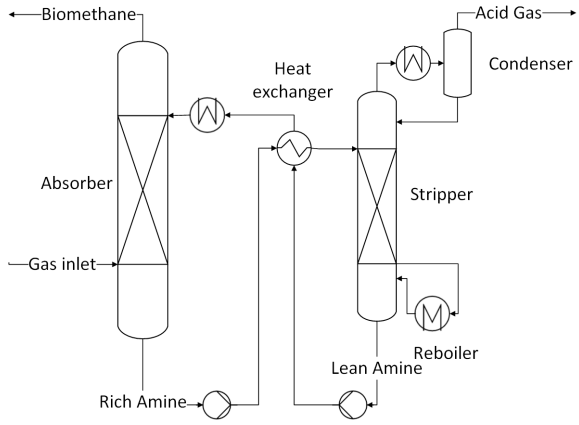

Figure 3.4: A simple process flow diagram of the base case.

.

3.3.2 Absorption Enhancement

The process modifications implemented are designed to increase the CO_2 loading at the absorber bottom or to reduce the excessive driving force in the absorber section. This reduces the solvent flow needed to achieve a given capture rate, which reduces the reboiler duty.

Intercooled absorber (ICA)

The principle behind the intercooled absorber is to remove a fraction of the solvent in the column, cool it down and re-inject it into the absorption column. This causes a shift in the thermodynamic gas-liquid equilibrium. As a result the rich loading is increased at the absorber bottom, hence increasing the CO_2 capture. The increased capture rate reduces the solvent flow rate which reduces the reboiler duty in the stripper. The draw-back of this system is that the reduced temperature in the absorption column reduces the chemical kinetics and diffusivity. [32] stated that "the system is ideal for low-kinetic solvents such as tertiary amines and/or amine with large heat of absorption.", based upon this it can be expected that intercooling will have a larger effect on AMP compared to MEA systems.

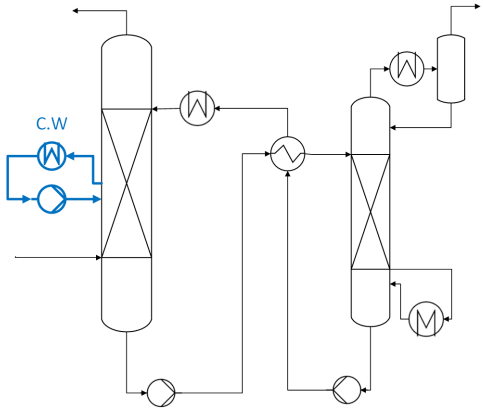

Figure 3.5: A process flow diagram of the intercooled absorber modification. Alterations to base case shown in blue.

.

In order to optimize the modification, the following parameters have to be considered,

1. Cooling position in the column
2. Temperature level of the cooled solvent
3. Fraction of solvent to be cooled
4. Lean loading

There are several possible solutions to the system. Heat integration can reduce/or eliminate the need for additional cooling water. The rich solvent out of the absorber can be used to reduce the temperature, this will again lower increase the heat transfer in the heat exchanger, and leading to an overall more efficient process. Multiple cooling steps has been suggested in order to achieve the optimal

thermodynamic conditions in the absorption column. For activated AMP a reduction in reboiler duty of 7% was found by [35]. For MEA a reduction between 1-6% has been found for coal fired power plant loss efficiency [27, 28, 29, 34].

Rich solvent recycle (RSR)

The purpose of the rich solvent recycling is to remove a fraction of the rich solvent out of the absorption column, and inserting it to the higher levels of the column. This modification enhances the absorption, by increasing the contact time between CO_2 and the solvent, thus increased use of the amine potential loading. This will allow the system to use less solvent. This modification is especially relevant for slower reacting solvents, such as tertiary amines. As stated for ICA, it is often beneficial to cool a fraction of the solvent removed from the column before re injecting it. Hence, this modification is often coupled with the ICA. 7% increase in rich loading and 5% reduction in overall energy consumption compared to the base case is stated by [36].

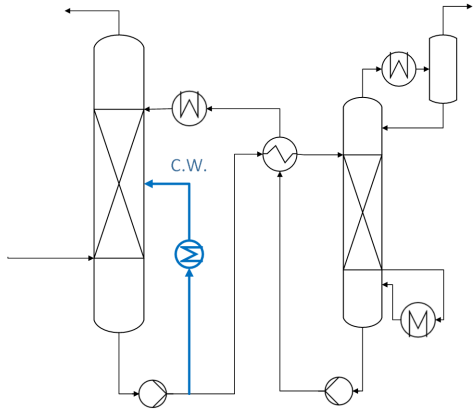

Figure 3.6: A process flow diagram of the rich solvent recycle modification.

.

Feed gas compression and expansion (FCE)

The purpose of the modification is to increase the driving force of the absorption, by increasing the pressure and thus the partial pressure of CO_2. There will be higher rich solvent loadings, hence use of less reactive solvent can be expected by implementing this system. By reducing solvent flow, the required heat in the stripper column is reduced. The increased driving force by increased partial pressure of CO_2 is restricted by the diffusion of the reactive amine [37]. The cost of compression can be reduced by sending the outlet gas from the absorber into a turbine. The outlet gas has been heated by the exothermic reactions in the absorber, in ad-

dition, heat sources found else where in the process, such as the stripper outlet, can be used to heat the gas further before expansion. An important aspect of FGC is the outlet pressure of the purified gas. For flue gas CO_2 removal, the purified gas i typically released to the surroundings. In this case, energy can be reclaimed by expansion of the purified gas as mentioned above. For biogas on the other hand, the product biomethane stream is typically pressurized before further use. In this case, the elevated pressure is directly utilized in the process.

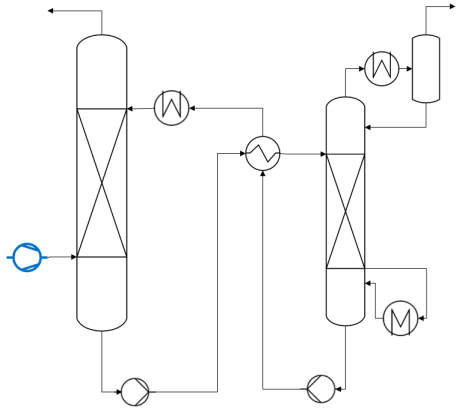

Figure 3.7: A process flow diagram of the feed gas compression modification.

.

3.3.3 Heat Integration

The general idea of heat integration is to minimize the heat loss from the system by transferring heat from the different process streams. This will result in lowering the required reboiler heat duty. A highly integrated system can ensure that the potential of the heat invested in the system is well spent, however a highly integrated system requires more process equipment and increases the cost.

Rich solvent splitting (RSS)

The modification involves splitting the rich stream into two flows; the largest stream is preheated in the heat exchanger as the conventional setup the second stream is kept cold. The cold stream is injected above the heated stream. This arrangement allows the temperature profile in the stripper to be smoothed, this increases the heat recovery, hence reduces the reboiler duty. The setup exploits the energy in the vapor leaving the column. In the conventional setup the vapor is sent from the column to the condensator with no benefit. By inserting a cold fraction of the rich stream higher in the column, the energy carried by the hot vapor out is reduced. This also reduces the cooling duty required in the condenser.

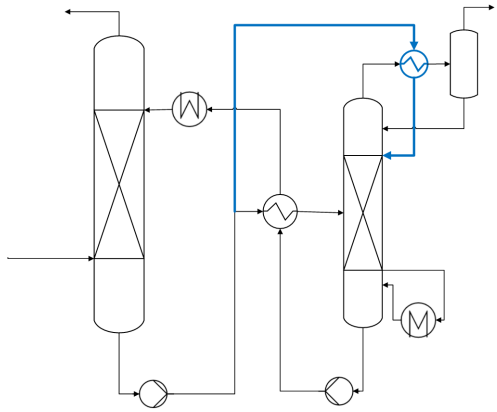

Figure 3.8: A process flow diagram of the rich solvent splitting modification.

.

Common variants involve heating of the cold fraction of the rich stream. The heat can be provided by the vapor stream leaving the stripper. For CO_2 removal from flue gas application, RSS can lead to 10-12% reduction in the reboiler heat demand [27, 28, 30, 31].

3.3.4 Heat Pumps

The purpose of these process modifications is to increase the quality of the heat by a heat pump effect. The additional heat made available is supplied at the costs more mechanical work. This enables an increased quality of available heat, which may reduce the overall heat energy demand.

Lean vapor compression (LVC)

The pressure of the lean solvent at the bottom of the stripper is reduced and the stream entered into a flash drum. The gasous stream from the flash is then compressed and fed back to the stripper. The compression of the gas increases the temperature before entering the stripper. This reduces the demand for heat in the reboiler. The temperature of the lean solvent leaving the stripper is lowered as a result of the decreased reboiler duty. This reduction results in a decreased temperature rise for the rich solvent in the heat exchanger. Hence the temperature in the top of the stripper is reduced. As a result less heat is lost in the stripper condenser. Lowering the stripper temperature will also have a positive effect on amine degradation. The effects of LVC was found to be as high as 23.7% from a study on CO_2 removal from a cement production with gas containing 30[vol%] CO_2 [38].

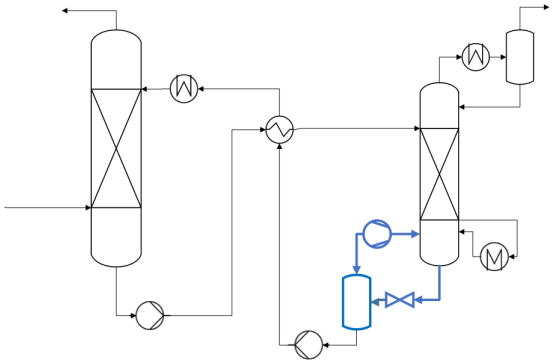

Figure 3.9: A process flow diagram of the lean vapor compression modification.

.

Rich vapor compression (RVC)

The principle of the modification is to flash the rich stream into a gasous stream and a liquid stream. The gasous stream is compressed to the appropriate stripper pressure, this increases the temperatur of the gas, which reduces the reboiler duty in the stripper. The advantage, as it turns out, is that the mechanical work needed for the compression is less than the reduction in heat needed in the stripper by the introduction of compressed gas. The gasous stream is routed to the bottom of the stripper column, whereas the rich liquid stream is inserted to the top.

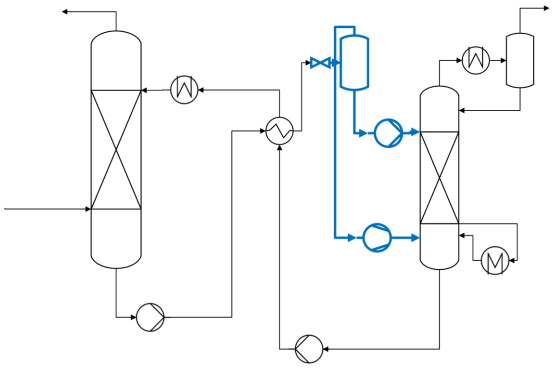

Figure 3.10: A process flow diagram of the rich vapor compression modification.

.

After the pressure reduction in the flash tank, the temperature of the fluids are reduced. The temperature of the gasous stream is elevated upon compression. The liquid stream can be heated further by an additional heat exchanger prior to the original heat exchanger, also utilizing the heat provided by the hot lean amine

stream out of the bottom of the stripper column. This reduces the heat transfer in the first heat exchanger. Hence reducing the temperature loss by not excessively elevating the temperature of the rich stream before it enters the flash tank. This has been patented by [39].

3.3.5 Summary of Modifications

Previously published studies have introduced several ideas for improvement of processes removing CO_2 from another mixture of gases. The primary focus of these studies has been the removal of CO_2 from low pressure combustion flue gases from power generation. The published literature contains relatively few experimental studies. Furthermore, the studies include a large scatter of conditions, gas compositions and performance objectives. Few studies have made attempts to systematically consolidate the information. Moreover the published studies are mainly limited to MEA. [35] found that the implementation of ICA reduced the reboiler duty with 7% for AMP+Pz, however the reported reduction was insignificant for MEA. The opposite was found for LVC, where a 20% reduction was found for MEA and only 13% for AMP+Pz. This indicates that the process modifications should be systematically compared to other studies with similar solvents, such as primary, tertiary and hindered amines etc. The reduced energy consumption should be evaluated against the cost of implementation and increased process complexity. In the study by [33] the total cost of implementation was evaluated against the amount CO_2 captured. Based on their methodology they established that in the case of heat exchanger configuration, a smaller temperature approach, with a corresponding increased energy savings, significantly increased the cost of captured CO_2. This highlights the importance of economic evaluation of implementation of process modifications. One should also consider the aspect of possible heat integration with other parts of a plant which may significantly influence the cost of heat/energy.

Chapter 4

Simulation Model of the CO_2 Absorption/Desorption Process in Aspen Plus

4.1 Pilot Campaign Simulated in This Thesis

The pilot used for validation of the simulations was based on the study by [40, 41]. The experimental setup was identical to that of [42], with a complete absorption/desorption pilot scale apparatus. The pilot was designed to be operated on a continuous basis. The pilot was designed with a 150 [Nm^3/h] gas treating capacity, but most of the runs were carried out with a gas flow of 120 [Nm^3/h] due to flooding issues in the absorption column. The pilot was designed as a closed system, thus all matter remained within the system. 11 runs were performed with different loadings, inlet gas conditions and operating temperatures. The specifics of the pilot are stated in Table 4.1. Other pilots evaluating AMP include [43, 44] and the studies validate both random and structured packing in the columns with both studies using 2M AMP solution. The pilot study by [44] was lacking temperature profiles and inlet and outlet temperatures for gas and liquid streams. The maximum temperature of the [44] study was 29 [°C], which is much lower than the expected industrial temperature of 40 [°C], possibly even as high as 65 [°C].

Table 4.1: Characteristics of the simulated pilot from [40]

Absorber Characteristics	
Column internal diameter[m]	0.15
Main packing height[m]	4.36
Packing type	Sulzer Mellapak 250Y
Desorber Characteristics	
Column internal diameter[m]	0.1
Main packing height[m]	3.89
Packing type	Sulzer Mellapak 250Y
Reboiler[m]	Ø0.40*0.80(D*L)
Liquid circulation rate(l/min)	3-6
AMP concentration(mol/m3)	2830-2890
Rich solution loading(mol/mol)	0.151-0.479
Lean solution loading(mol/mol)	0.072-0.389
Inlet CO_2 concentration([vol%])	2.38-12.96

4.2 Aspen Plus Template

The CO_2 absorption/desorption was simulated in steady state with Aspen Plus V8.6 using the template "ELECNRTL_RATE_BASED_AMP_MODEL". This model is applied for rigorous modelling of electrolyte species, according to Aspen Plus the applicability range is given for AMP concentrations up to 28.5[wt%] and temperature in the area 40-100 [°C]. The property method used in the template is the "non-random-two-liquid"(NRTL). The ELECNRTL is an activity coefficient property method, and uses the Soave Redlich-Kwong equation of state as the vapor phase fugacity coefficient method, and Electrolyte NRTL as the liquid phase activity coefficient method. The ELECNTRL is stated by Aspen Plus as the recommended property method for acid gas absorption. The AMP template includes the required physical properties and reaction parameters to simulate the AMP/H_2O/CO_2 system. For the deveopment of this thesis the properties established for the involved compounds were used without changes.

The absorber and the desorber columns in the template are determined as RadFrac, which is a column type in the Aspen Plus model bank designed for general vapor-liquid multistage separation. The absorption was selected as a Rate-Based model, which performs rate-based, non-equilibrium separation. With this setup, the column is simulated as a actual packed column rather than a idealized rep-

resentation. The Rate-Based modelling in Aspen Plus evaluates mass and heat transfer in the separation process. This yields a more accurate representation of the column, and requires more computational effort. Bravo et al. (1985) was used for the mass transfer coefficient method and the interfacial area method. The heat transfer correlation was taken from Chilton and Colburn [55].

4.3 Absorber and Desorber Column Stages

The number of stages set for the absorption and desorption columns in Aspen Plus, determines the discretization of the columns, i.e. how many calculations to solve the column. Increased number of stage should yield a more accurate result, but requires more computational effort. The number of stages for the absorber and desorber were determined based on evaluation of the relative change by increasing the number of stages. The solutions for a given simulation should converge, eventually leading to negligible change by increasing the number of stages. The evaluation of required number of stages is shown in Figure 4.1. It can be seen that the computational effort and relative change in simulation results for increasing number of stages is much smaller for the desorption column, simulated with the equilibrium method. The satisfactory number of stages was set as 20 and 10 for the absorption and desorption column respectively. The number of stages were then kept constant for the duration of the presented study.

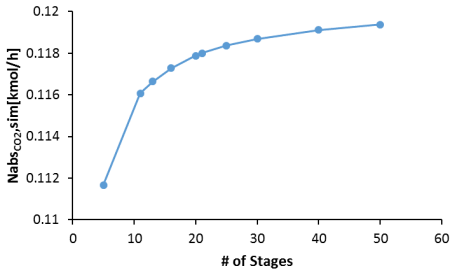

(a) Absorber

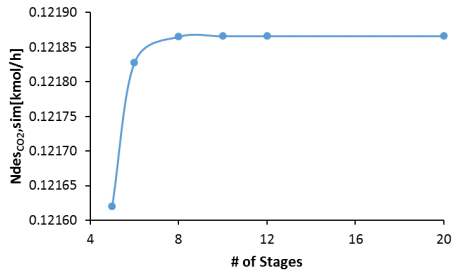

(b) Desorber

Figure 4.1: Figures showing the evaluation of required number of stages in simulation for Rad-Frac columns. The absorption column is simulated with a rate-based model, and the desorption column with a equilibrium based model.

For the absorption column, the inlet solvent stage feed was set as the 1 and the inlet gas stream was set as 20, being the top and bottom respectively. The feed was fed "on-stage". This specification determines that the feed is fed to the specified stage. This determines the flash calculation when feed enters the column.

Using "above-stage" causes the vapor phase to go directly to the above stage, and the liquid phase to the below, without flash calculations. The inlet solvent stream was determined as "liquid only", this means that Aspen Plus treats the stream as a single phase flow, this eases the computational effort. The inlet gas flow was specified as "vapor-liquid", hence Aspen Plus allows to compute a two phase flow. The rich outlet solvent was exiting at stage 20, and the purified gas at stage 1. A print screen from Aspen Plus showing the process flow diagram of the absorption column is show in Figure 4.2 below.

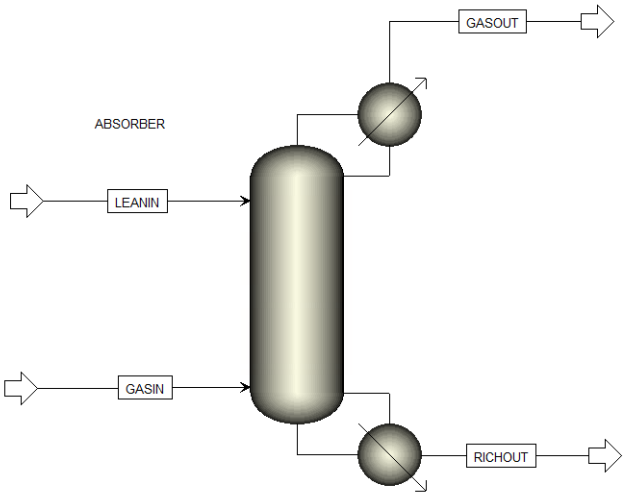

Figure 4.2: A screen shot of the process flow diagram from Aspen Plus.

.

The desorption column was simulated with 10 stages and an equilibrium model. The rich solvent was fed at stage 1, and set to the Aspen Plus default "vapor-liquid". The Rich gas stream exited the column at stage 1 and sent to a condenser, simulated as an external flash tank. The rich CO_2 stream was routed into a condenser, and the condensed liquid stream was recycled to the desorption column at stage 10. The lean solvent left the column at stage 10. The reboiler was located at the bottom of the column in stage 10. With the setup with an external condenser and a reboiler at the bottom, the desorption column could be specified with a single variable, chosen as the reboiler duty. An illustration of the simulation model of the desorption column in Aspen Plus is shown in Figure 4.3

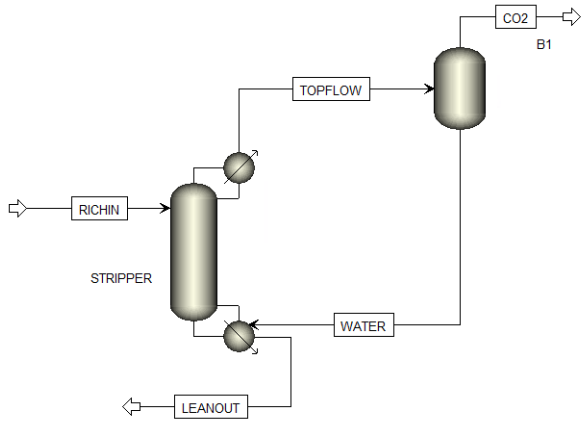

Figure 4.3: A simple process flow diagram of the desorption pilot plant.

.

4.4 Vapor Liquid Equilibria

Several concentrations of AMP were investigated in order to find a good fit with the available experimental data. The experimental data used for comparison of the results from the present study are listed in Table 4.2.

Table 4.2: Overview of literature used in comparison of model and experimental data.

	Data sources	Year	Temperature range		Concentration [M]		
			Low	High	Low	-	High
1	Dash et al.[45]	2011	298	328	2.8		4.9
2	Kundu et al.[19]	2003	303	323	2		3.4
3	Li and Chang[46]	1994	313	373		3.4	
4	Seo and Hong[18]	2006	313	353		3.4	
5	Silkenbäumer et al.[47]	1998	313	353	2.4		6.45
6	Teng and Mather[48]	1990	313	343		2	
7	Tong et al.[49]	2012	313	393		3.4	
8	Tontiwachwuthikul et al.[50]	1991	293	353	2		3

The different results for the vapor liquid equilibrium simulations are shown in Table A.1 in Appendix A, where the deviations have been calculated according to the equations shown in Appendix B. It can be seen from Table A.1, that the specific range given in Section 4.2 correlates well with the present results, whereas the experimental and simulated results correlate poorly for temperatures and loadings outside of the specified range.

Vapor liquid equilibrium (VLE) curves for CO_2 in the concentration and temperature range stated in Table 4.2 were generated in Aspen Plus. Flash tank simulations were used to examine the models ability to predict the vapor liquid equilibrium. The operating characteristics are determined by the VLE, hence a good correlation should be achieved in order to ensure the accuracy of the simulations. The simulation results were compared to the experimental data by sources given in Table 4.2. The VLE results for 30[wt%](∼3.4M) AMP are shown in Figure 4.4. Graphic representation of the other VLE simulations are not given in this report, as 3.4M was used for further work.

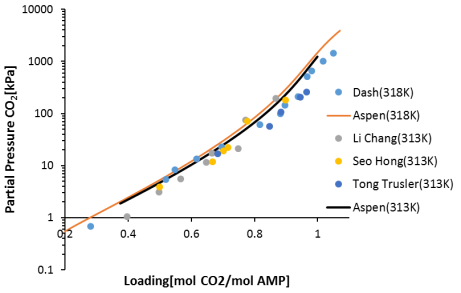

(a) 40°C

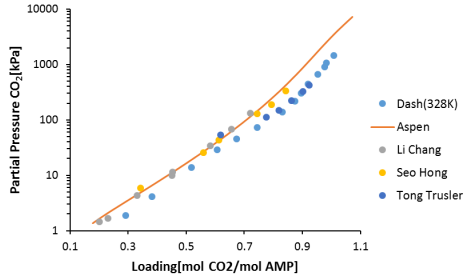

(b) 60°C

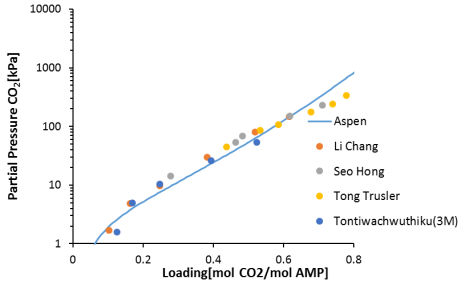

(c) 80°C

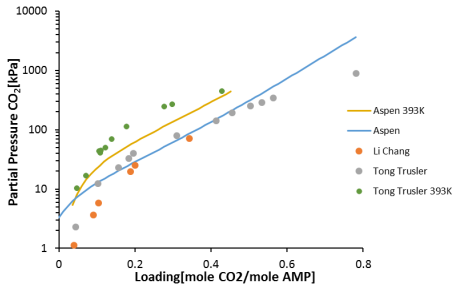

(d) 100°C and 120°C

Figure 4.4: Figures showing VLE simulations for 3.4M AMP for different temperatures. Comparing simulation results and experimental values.

It can be seen from Figure 4.4 that the predictions of the simulation model are in good agreement with experimental data. Although Figure 4.4(d) indicates that for temperatures above 120 [°C] there are larger differences compared to those within the application range of 40-100 [°C]. From this it can be expected that for strippers operating below 120 [°C] there will be more accurate results, at least consistent with experiments. The VLE behaviour of the simulated AMP/H_2O/CO_2 system was considered sufficiently precise for simulation of the absorber and stripper.

Chapter 5

Comparing Experimental and Simulated Pilot Data

5.1 Absorber Simulations Setup

The following experimental data was used to compare the experimental and simulated data:

- Gas and liquid feed to absorber: molar flow rate (F), component molar fraction (x_i), temperatures (T) and pressures (p).
- Outlet gas and liquid streams from absorber: molar flow rate (F), component molar fraction (x_i), temperatures (T) and pressures (p).
- Temperatures through the packing to establish temperature profiles.

The conditions of the feed streams to the absorption column were established as the inputs for the absorber simulation model. Data recorded from the simulation are stated in the list above. The absorption rate of CO_2 from the simulation was compared to absorption rate from experimental data. This established the basis for the performance validation. The liquid phase was used as basis for calculating the absorption rate. The absorption rate was used to calculate the deviation according to Appendix B.

5.2 Absorber Simulations

The template provided by Aspen Plus was firstly applied without alterations, except for the inlet conditions and column design specified in the pilot by [41] as stated in Table 4.1. In an attempt to improve the simulation model, modifications to the kinetic constant was tried. This were done by altering the pre-exponential factor and the activation energy in the Arrhenius equation used in the Aspen Plus kinetic model, shown in Equation 5.1.

$$k = Ae^{-E_a/RT} \tag{5.1}$$

where k is the reaction rate constant, A is the pre-exponential factor, E_a is the activation energy, R is the universal gas constant and T is the temperature. However the changes yielded little reduction of the deviation. It was therefore decided to use the template without alteration.

5.3 Absorber Simulation Results

The experimental data collected by [40] consisted of 11 runs with three ranges of lean loading. Run 1-4, with lean loading of 0.072-0.118, Run 5-7, with 0.142-0.170, and Run 8-11, with 0.219-0.309. Figure 5.1 shows a decreasing trend of the absorption rate with loading. This mean that the simulation model is overestimating the rate of absorption for lower loadings and underestimating the absorption rate for higher loadings. For the other plots there is no clear indication of a pattern. The results of the absorption simulation is shown in Appendix C. The AAD and AD were calculated to 12.8% and 12.7% respectively. This deviation between the simulated data the experimental data is considered satisfactory.

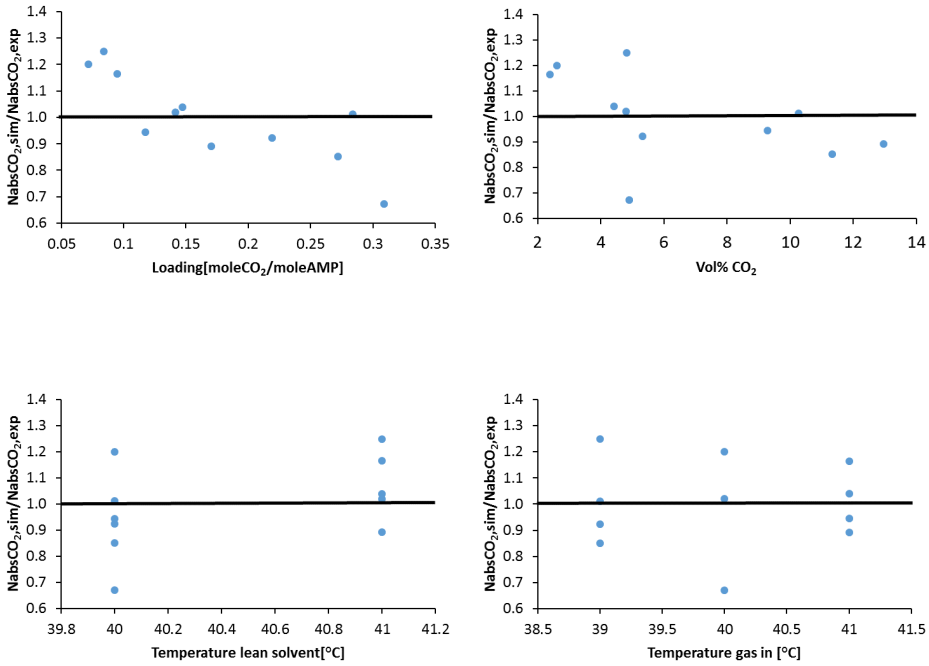

Figure 5.1: Figures showing comparison of experimental and simulated values for the absorption column.

The temperature profiles from the model were compared to temperature profiles of the pilot column. Three runs where evaluated on the basis of the argumentation by [41] with three different loading ranges and quite large CO_2 flux. It was found that Run 11 yielded less good results as those with lower lean loadings. Hence, run 11 was compared as a second comparison from the higher loading range. Figure 5.2 shows the comparison of the experimental and simulated temperature profiles.

From Figure 5.2 it can be seen that the temperatures of the simulation model is lower than the experimental values, especially around the temperature bulge, which is where most of the absorption takes place. However the agreement between simulated temperatures is good for most of the runs. The agreement for the temperature profiles was a bit unexpected since the simulation model both underestimated and overestimated the absorption. One may expect the temperature to be overestimated for the low lean loadings, were the absorption was overestimated, and a underestimation for higher lean loadings were the absorption was underestimated. A good explanation was not found for the relative larger temperature deviation for Run 11.

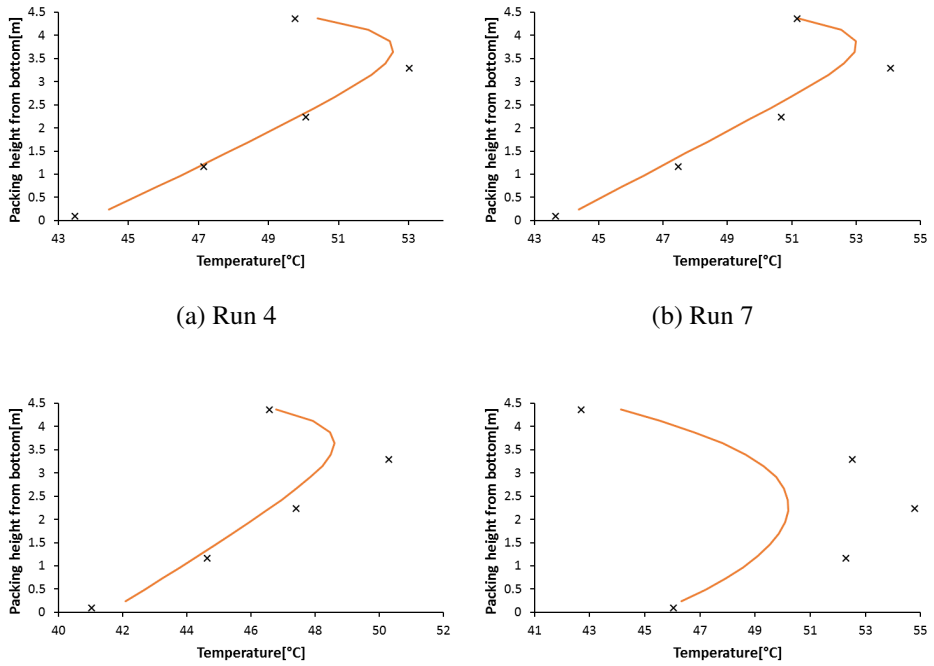

(a) Run 4

(b) Run 7

(c) Run 10

(d) Run 11

Figure 5.2: Figures showing temperature profiles for the absorption column. Experimental values are marked with x, and simulation shown as the red line.

5.4 Desorber Simulations Setup

The following experimental data were used to compare the experimental and simulated data:

- Rich solvent fed to stripper: molar flow rate (F), component molar fraction (x_i), temperatures (T) and pressures (p).
- Outlet gas and liquid streams from stripper: molar flow rate (F), component molar fraction (x_i), temperatures (T) and pressures (p).
- Temperatures through the packing to establish temperature profiles.
- Reboil duty (Q), condenser temperature (T) and pressure (p).

The input of the desorber simulation was the inlet rich solvent stream and the reboiler duty. The outlet flows and temperature profiles was compared to the experimental data.

The deviation were calculated according to Appendix B and the performance of the desorption model evaluated. The desorption rate was taken from the molar flow of CO_2 in the gasous stream leaving the system.

5.5 Desorber Simulations

The desorber was based on the description by [16] and data from [40]. The Aspen template was used as the basis for simulations. The reaction rates in the desorption process is very fast, hence the equilibrium model was used to simulate the column. The desorption simulation was found to under-predict the stripping compared to the experimental data. As a result heat loss to the surroundings was not included in the model, which would only decrease the stripping further and be dependent on the thermal insulation of the column. An illustration of the simulated pilot is shown in Figure 4.3. The AAD and AD was calculated to 8.0% and 14.1% respectively, shown in Appendix 2.2(b) This was deemed satisfactory.

5.6 Desorber Simulation Results

Figure 5.3 shows the simulated data for the stripper compared to the experimental data. It can be seen that the model exhibits a general underestimation of the desorption rate. However, no systematic trend can be derived from the plots as to a possible reason, as the results seems randomly scattered. The VLE results stated in Figure 4.4(d), Section 4.4 show that for the temperature of 100 [°C] and loadings less than 0.1, the simulated vapor pressure is less than the experimental values. However, the simulated lean loadings varied from 0.06 to 0.31, hence this is not sufficient to give conclusive reason.

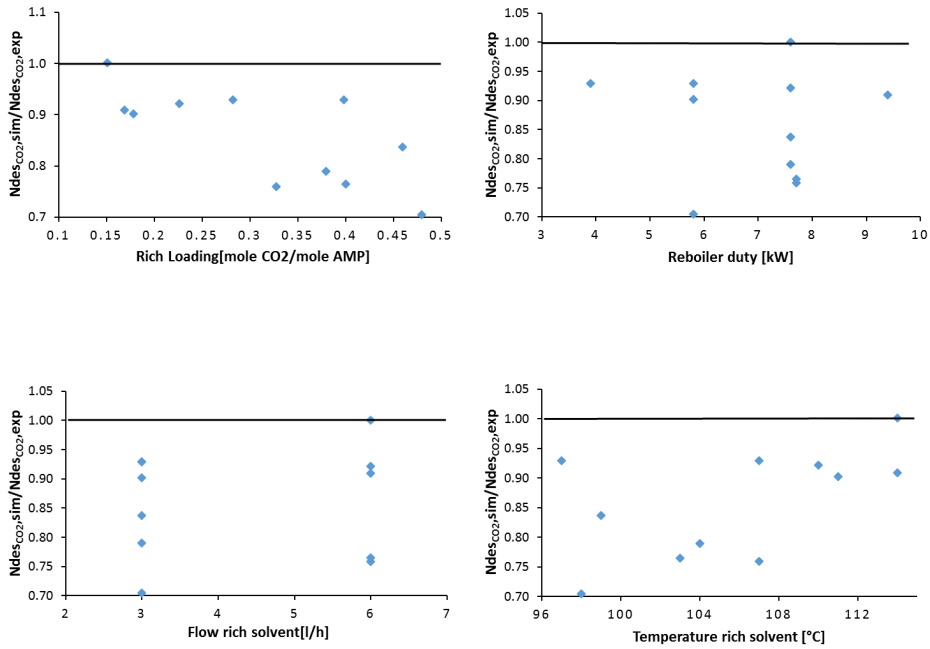

Figure 5.3: Figures showing comparison of experimental and simulated values for the desorption column.

From Figure 5.4 it can be seen that the match between the simulated and experimental results show significant deviation. However, the temperature profiles are in good agreement with the simulation results seen in Figure 5.3, since lower temperatures means a lower driving force for the stripping, hence reduced desorption rate.

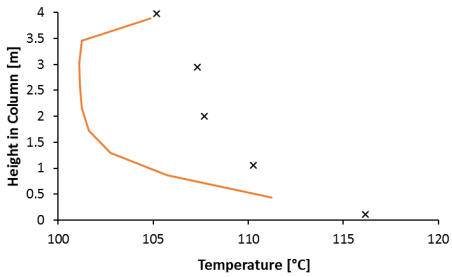

(a) Run 4

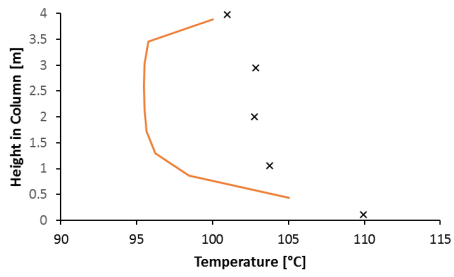

(b) Run 7

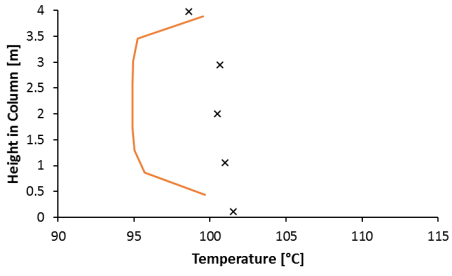

(c) Run 10

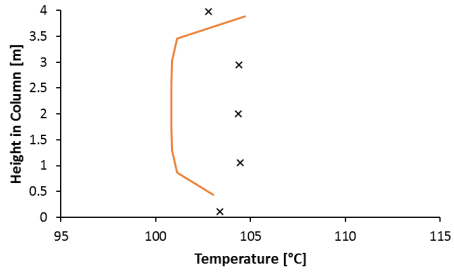

(d) Run 11

Figure 5.4: Figures showing temperature profiles for the desorption column. Experimental values are marked with x, and simulation the red line.

In order to better represent the temperature in the desorption column, the template was examined. The reactions specified in the desorption column was by set to the reactions defined in Table 2.1. Because of the fast reaction regime, the stripper was specified with the equilibrium calculation method, the kinetic reactions in Table 2.1 was therefore specified as equilibrium reactions only, in the simulation model in Aspen Plus. This change yielded the temperature profiles seen in Figure 5.5.

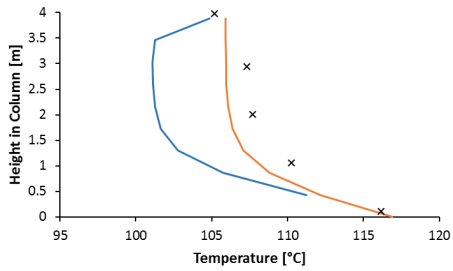

(a) Run 4

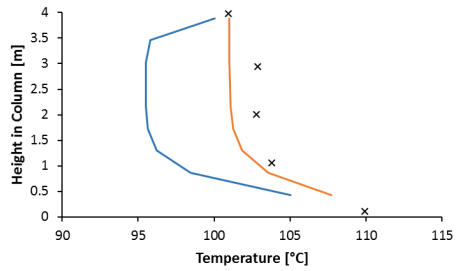

(b) Run 7

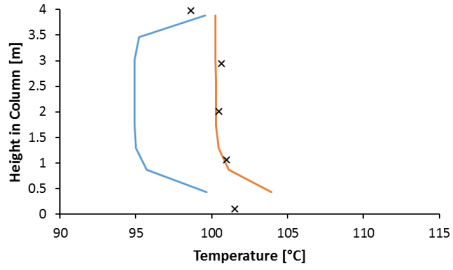

(c) Run 10

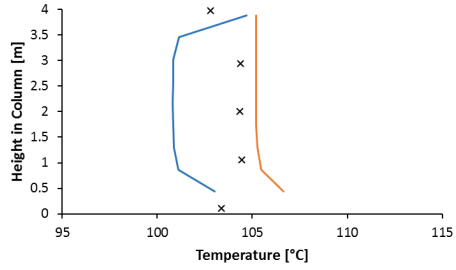

(d) Run 11

Figure 5.5: Figures showing temperature profiles for the simulation of the altered desorption column. Experimental values are marked with x, and the updated simulation the red line. The unchanged template is shown with the blue line.

It can be seen from Figure 5.5 that the changes in the reactions imposed better representation of the temperature profiles in the column. The positive effect did however not, have a significant effect on the desorption rate. The AAD and AD were found to be 7.1% and 17.0% respectively. Because of the better temperature representation, it was decided to use the updated kinetics for the desorption column for further simulations.

Chapter 6

Input Structure of Base Case and Process Modifications

6.1 Energy Calculation

Heat, electricity and/or mechanical energy are the main energy inputs of the process. Heat for the reboiler and electricity or mechanical energy for the pumps and compressors. The energy of these two types have different exergy values and cannot be unified directly. This work has chosen the same method as [34], where the heat required is converted to equivalent thermodynamic work, i.e how much electricity can be produced with the same amount of steam for the reboiler.

[34] make use of Equation 6.1 in order to calculate the total equivalent work for the plant.

$$W_{eq} = Q_r \left(1 - \frac{T_C}{T_H}\right) \times \eta + W_{Pumps} + W_{Compressors} \tag{6.1}$$

where the temperature of the steam in the reboiler T_H is assumed to be 10 [°C] higher than the reboiler temperature, hence $T_H = T_{Reb} + 10$ [K], and that the steam condenses at 40 [°C] in the turbine $T_C = 313$ [K]. The turbine efficiency η was assumed to be 75%.

For optimum operation of biomethane production, most of the electricity and heat is typically provided by an on-site combined heat and power (CHP) plant [51]. Further on [51] found from cases studies that the thermal energy conversion of these CHP installations typically was in the range from 45-50%, similar for small

scale plants [52]. A Danish study [53] stated a typical conversion factor of 45-60% for thermal energy conversion for biogas for CHPs. For the purpose of this report it is assumed on-site CHP installation with thermal conversion of 50%.

Fired heaters are also common for biogas upgrading plants to provide the heat needed in the plant. Biogas can potentially be utilised directly in heaters without upgrading, but with some conditioning. Modern fired heaters operate at thermal efficiencies of between 80-90%[54]. Depending on the fuel and the excess air requirement. This was however considered outside the scope of this thesis.

6.2 Base Case

In order to establish the relative change in the system by implementing the selected process modifications, a base case was established as a basis for comparison. The Aspen Plus model developed for the base case was based on the description of a general amine absorption process, see Section 2.1, and findings from the absorber and desorber pilot simulations. In addition to the conventional process description, it was decided to implement a flash tank between the heat exchanger and the rich solvent inlet to the stripper. This reduced the phases in the rich solvent feed into the stripper to liquid only, hence reduced the computational effort for the initial flash calculation in the column. This is known as "rich solvent flashing" and can be implemented as a modification to improve the system performance. The vapor stream out of the flash tank was mixed with the stripper vapor outlet flow and sent to the condenser. A print screen of the base case process flow sheet in Aspen Plus Plus is shown in Figure 6.1.

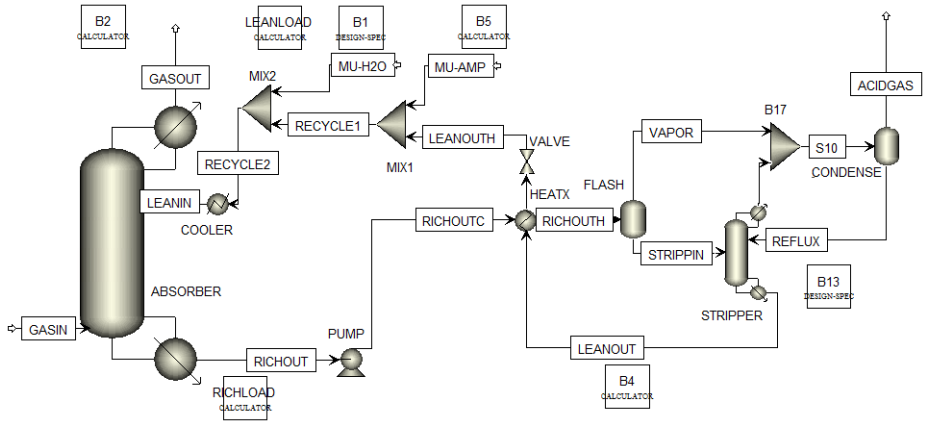

Figure 6.1: A print screen of the base case established in Aspen Plus

.

6.2.1 Input structure

The heat exchanger was specified as a counter-current shell and tube heat exchanger. The temperature difference between the hot outlet and the cold outlet was set to 8 [°C], which was considered reasonable. This approach was also applied to achieve a robust approach to convergence and a flexible model. Operating too close to pinch could be problematic when implementing several modifications and tuning the operation of these. The flash tank between the heat exchanger and the stripper column was operated at the same pressure as the stripper, 2 [bar] and zero duty. The condenser was operated at 12 [°C] and 2 [bar].

The make-up streams ensured that the mass balance in the system was constant by adding the same amount of new solvent to the system as was lost from the outlet streams "GASOUT" and "ACIDGAS". MU-AMP added new AMP to the system according to the measured losses in the outlet streams. The lean solvent in "LEANIN" on the absorber was defined as a tear stream with a given flow rate and composition. Tear streams are defined by Aspen Plus as streams to calculate the convergence of recycle loops. Water equal the required mass to ensure mass balance was maintained in the system by the MU-H2O stream seen in Figure 6.1. The amount of water was determined by a design specification block, which calculated the mass difference between the recycle loop and the tear stream (LEANIN). A second design specification block ensured the amount of CO_2 leaving the system was constant. The block regulated the amount of CO_2 leaving in gaseous stream from the condenser, by changing the reboiler duty in the stripper.

6.2.2 Convergence

It was found that the default settings for the Aspen Plus template needed to be altered in order to achieve convergence when the recycle loop seen in Figure 6.1 was activated. First attempts to converge the system were made by ensuring that the LEANIN defined as a tear stream, was close in mass and composition for both ends of the loop, before the loop was closed. In order to converge the system the different convergence methods used by Aspen Plus, such as Wegstein, Broyden, Newton and direct secant method were applied and tuned according to the Aspen Plus Manual [55], it was found that the problem was not associated with the convergence method. The main issue was with the calculation of tear streams, defined in Aspen Plus as streams to be converged by a convergence block. These must be in recycle loops in the simulation flowsheet. The tear streams were specified to converge outside other convergence block, and design specifications to converge with tear streams. The tolerance of the tear stream convergence was increased from 1 e-03 too 1e-04. With the mentioned tear stream changes the system converged. The convergence methods were kept as default setup as seen in Table 6.1.

The stream defined as in the system as tear streams was: LEANIN, REFLUX and STRIPPIN.

Table 6.1: Convergence method setup in Aspen Plus

Default convergence methods	
Tears	Wegstein
Single design spec	Secant
Multiple design spec	Broyden
Tears and design spec	Broyden
Optimization	SQP

6.2.3 Operating Conditions

Table 6.2: Operating conditions stated for base case and process modifications

Absorber		
Column Diameter	[m]	0.15
Packing Height	[m]	15
Packing Type	-	Sulzer Mellapak 250Y
Operating Pressure	[bar]	1
Stripper		
Column Diameter	[m]	0.1
Packing Height	[m]	3.89
Packing Type	-	Sulzer Mellapak 250Y
Operating Pressure	[bar]	1
Flow Specifics		
Biogas Flow Rate	[kg/h]	13.4
Biogas Flow Rate	[Nm^3]	12.0
Lean Solution Flow Rate	[kg/h]	119-303
Lean Solution Loading	[mol CO2 /mol AMP]	0.002-0.311
Rich Solution Loading	[mol CO2 /mol AMP]	0.413-0.630
CO_2 biogas in (dry basis)	[mol%]	40
CH_4 biogas in (dry basis)	[mol%]	60
Pressure CO_2 biogas in	[bar]	2
CH_4 biomethane out (dry basis)	[mol%]	97
Captured CO_2	[kg/h]	8.29
Temperature Biogas	[°C]	20
Temperature Lean Solvent	[°C]	40

The operating conditions for the base case and the process modifications are shown in Table 6.2. It was decided to reduce the column capacity to establish a flexible model that could work when implementing the process modifications, ideally without changing the operating conditions. Several factors where identified which could be problematic if the capacity was not lowered. Firstly, it was found that the pilot operated close to flooding conditions. Secondly, the removal of a considerable larger amount of CO_2 meant using higher solvent flow rates. Thirdly, operating at higher capacity meant less flexibility when implementing process modifications. The gas flow rate used in the pilot testing [40] for the absorption and desorption validation in Section 5.2 and 5.5, was reduced to 12 [Nm^3], which was found to be 20% of column capacity.

The gas flow fed to the column is an important factor for a contacting vessel. If the gas flow rate becomes to large it can lead to entrainment or flooding of the column. Flooding occurs when the resistance between the liquid film and the gas becomes large enough to stop the liquid from falling. Entrainment and increase in carry over occurs when liquid is transported out of the top of the column by the gas, when the gas flow rates becomes too large compared to the liquid flow rate. Typical operation conditions for the gas mass velocity is stated for absorption columns as 80% of flooding gas mass velocity [56, 57]. Figure 6.2(a) shows the reboiler duty as a function of absorber height. Figure 6.2(b) shows the specific heat requirement as a function of various liquid an gas flow rates, with constant L/G ratio.

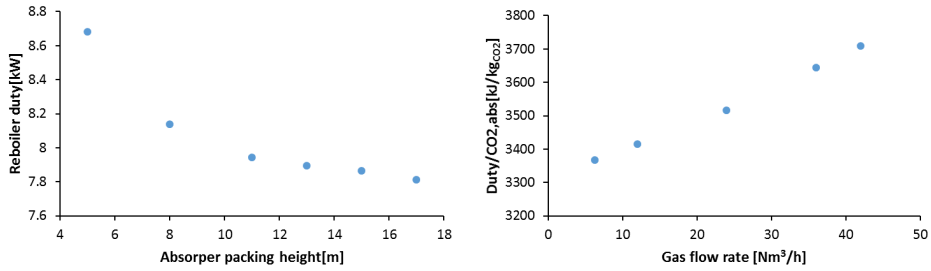

(a) (b)

Figure 6.2: a) Illustration of the reboiler duty versus the absorber height. It was found that the reboiler duty flattened out after a height of around packing 11[m]. b) Illustration of the reboiler duty versus the gas feed flow rate. The liquid to gas mass ratio was held constant as 20, with 30[wt%] AMP.

In Figure 6.2(b) the gas flow rate was increased up to approximately 80% of flooding capacity with constant liquid to gas mass ratio. The associated reboiler duty to maintain a constant CO_2 capture rate was recorded. The specific reboiler heat demand for separating CO_2 was found to increase for increased vapor gas flow rates in the column. Further investigation revealed that the cyclic loading was constant, but the lean and rich loading decreased for higher flow rates. The increase in specific energy required can be explained by higher reaction energy for lower loadings [26].

It was found that the absorption was increased by increasing the length of the absorption column and the reboiler duty reduced, shown in Figure 6.2(a). It was therefore decided to increase the absorber height to the proportions of the Tiller pilot [58]. This ensured that the limiting factor of the process was not the absorption column. The the variation of column height, the cyclic loading was constant, but the rich loading was increased as a result of increased contact time, hence increasing the lean loading accordingly. The reduction in specific energy for separating CO_2 can therefore be explained according to the statement above, for the increased flow rate. Where the loading range determines the reaction energy. It was not found any considerable changes by increasing the sizing of the desorption column, this was assumed to be a result of the very fast reaction regime.

Solvent Flow Rate

The solvent flow rate affects the reboiler duty. Higher solvent flow rates increases the energy input because more solvent needs to be heated, however more solvent increases the CO_2 uptake in the absorption column, hence reducing the required lean loading. This can be seen in Figure 6.3, where the reboiler duty increases sharply for lower L/G ratios, because of required low lean loadings. Increased reboiler duty can be observed for higher L/G ratios. The optimal solvent flow rate was determined by comparing the solvent flow rate against the reboiler duty, while the inlet gas flow, the amount of captured CO_2, and the purity specification were held constant. The ideal case being minimal flow rate and reboiler duty combined. Graphs of the L/G ratios plotted against the reboiler duties are shown in Figure 6.3.

The base case was initially simulated with 20[wt%] AMP. High liquid to gas loadings were experienced as can be seen in Figure 6.3(a). The result was unexpected when compared to other cases with chemical absorption. The purification requirement was reduced to 90[mol%] CH_4. This reduction caused the the capture energy to drop and the area of operation to widen, as can be seen in Figure 6.3(a). It was found that when reducing the purification requirement, lower L/G ratios were required, but still high.

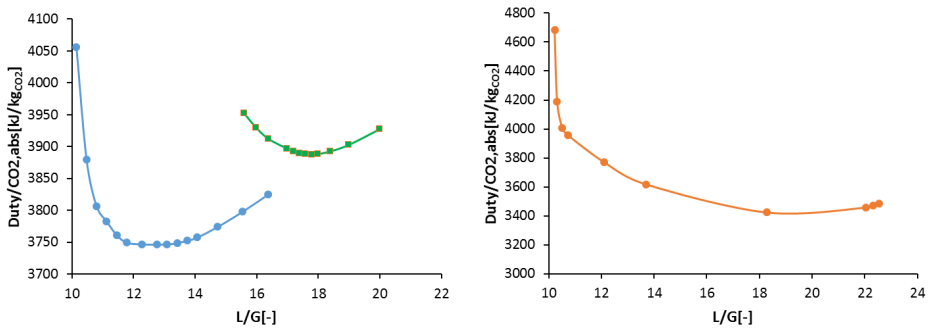

(a) 20[wt%] AMP

(b) 30[wt%] AMP

Figure 6.3: Liquid mass to gas mass flow rate plotted against the reboiler duty. Typical plots shows a U shaped curve which flattens at the bottom. The optimum flow rate can be found as the minimum flow rate before the reboiler duty sharply increases. Blue line, 20[wt%] AMP - 90% CH_4 in purified gas. Green line, 20[wt%] AMP - 97% CH_4 in purified gas. Orange line, 30[wt%] AMP - 97% CH_4 in purified gas.

The concentration of AMP was increased to 30[wt%] AMP in an effort to reduce the required solvent flow rate. The simulation results can be seen in Figure 6.3(b). Similar L/G flow rates and reboiler duties were found for the 30[%wt] AMP case. However, it was found by increasing the solvent flow rate that the energy requirement could be reduced and the area of operation became larger. From the literature survey, it was found that 30[wt%] is a common industrial concentration for AMP based systems. As a result of the above, 30[wt%] AMP was used for further investigations. The minimum observed in in Figure 6.3(b) with approximately 11 [kmol/h] solvent flow rate was used as a basis for the base case and the process modification cases.

Figure 6.4 shows the characteristics of the absorption column for different solvent flow rates, with constant gas flow rate and amount of CO_2 captured. As the solvent flow rate increased the cyclic loading decreases, as seen in Figure 6.4. This shows that when increasing the L/G ratio, more solvent is available to capture CO_2, but the capture potential of the solvent is less utilized. It can be seen from the temperature profiles in Figure 6.4 that for higher solvent rates, the temperature rise in the column is much smoother and lower temperatures are reached. This enables higher rich loadings seen in Figure 6.4. The uptake of CO_2 is much steeper in the column for lower L/G ratios.

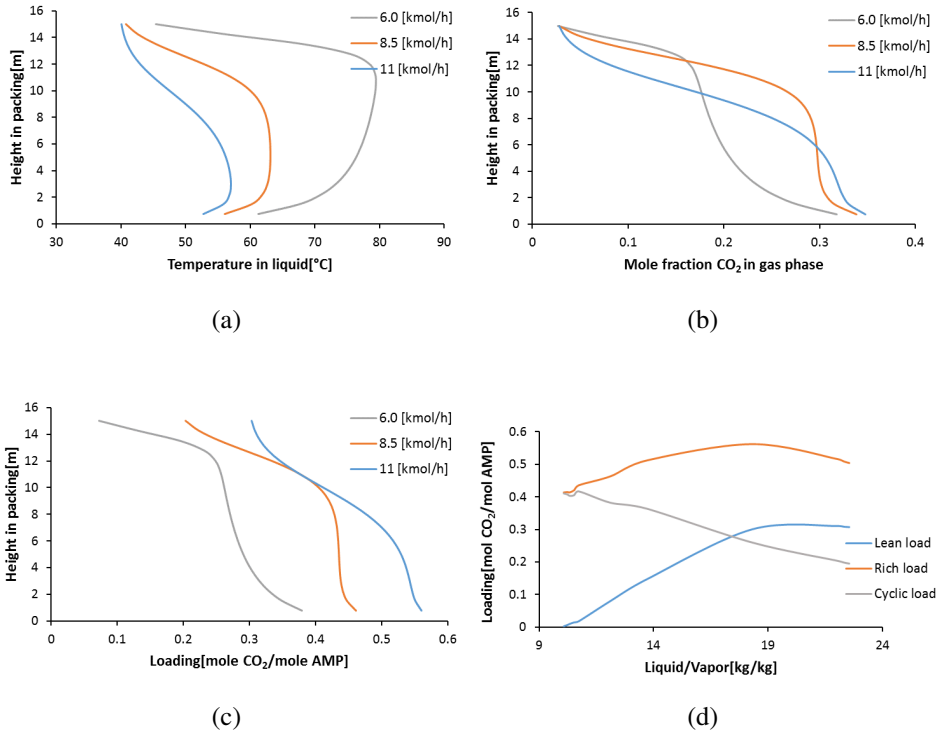

Figure 6.4: Illustrations of the characteristics for the absorption column for different solvent flow rates. Grey line: 6 [kmol/h]. Orange line: 8.5 [kmol/h]. Blue line: 11 [kmol/h]. Figure d) Loading for various liquid/gas flow rates. Rich loading given by red line, blue line giving the lean loading and the loading difference given by the grey line

6.3 Process Modifications

The operational conditions for the process modifications were the same as for the Base case, given in Table 6.2. The solvent flow rate for the modifications was the optimal flow rate found for the base case, 11 [kmol/h]. This flow rate was kept constant when each modification was evaluated with different alterations, such as split fraction etc. It was assumed that the relative differences would yield satisfactory results for pointing out the best tuning, without changing the solvent flow rate. When the best parameters was established for a modification, the optimal L/G ratio was determined, in order to establish the reduction or increase in solvent flow rate. Process flowsheets exported from Aspen Plus are shown for each modification in the subsequent sections.

6.3.1 Intercooled Absorber Setup

The intercooling was introduced as a side stream on the absorption column with a separate cooler. The solvent sent to the cooler was collected from the step above the insertion stage. Figure 6.5 shows the setup in Aspen Plus. The parameters which was changed in order to find the best implementation of the modification was: Split fraction, cooling temperature, and cooling stage. One parameter was changed, while two were held constant. As an example, when changing the cooling temperature, the split fraction and cooling stage were held constant at 0.2 and 12 respectively. This is shown in Table 6.3, where the constant parameters are given in bold.

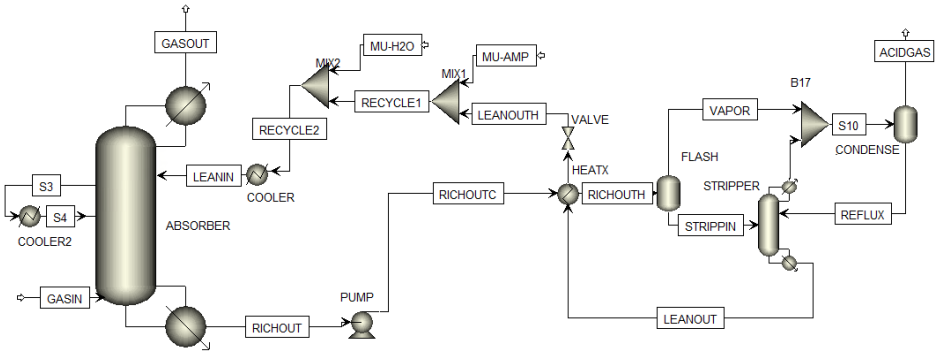

Figure 6.5: A screen shot of the process flow diagram from Aspen Plus for the intercooled absorber modification.

Table 6.3: Variations for intercooled absorber modification

Feed stage from top	9	**12**	15
Temperature [°C]	10	**25**	40
Split fraction	0.1	**0.2**	0.3

6.3.2 Rich Solvent Recycle Setup

A split was introduced on the rich solvent outlet of the absorber. This was sent to a cooler before injected back into the absorption column. In order to achieve convergence a small fraction was firstly extracted and recycled. The variables changes were the split fraction, cooling temperature and stage to feed the recycled stream. To evaluate the modification, the same variations were applied as for ICA, see Table 6.4. Figure 6.6 shows the setup in Aspen Plus.

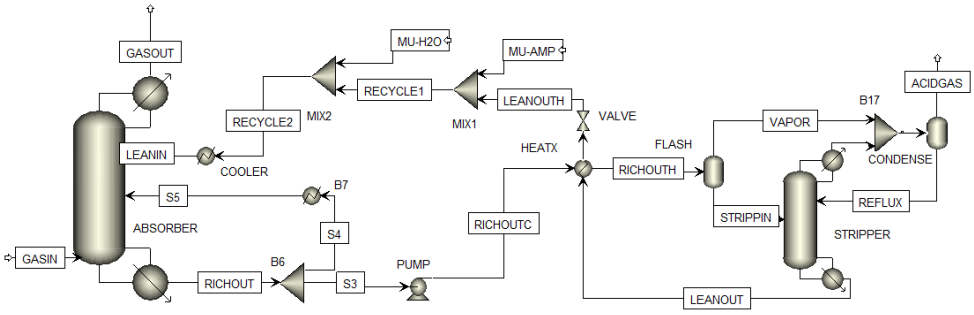

Figure 6.6: A screen shot of the process flow diagram from Aspen Plus for the rich solvent recycle modification.

.

Table 6.4: Variations for rich solvent recycle modification

Feed stage from top	9	**12**	15
Temperature [°C]	10	**25**	40
Split fraction	0.1	**0.2**	0.3

6.3.3 Feed Gas Compression Setup

A compressor was inserted on the gas feed stream to the absorber. A cooler was installed after the compressor to allow the compressed gas to be cooled down to 40 [°C] before entering the absorption column. Figure 6.7 shows the setup in Aspen Plus.

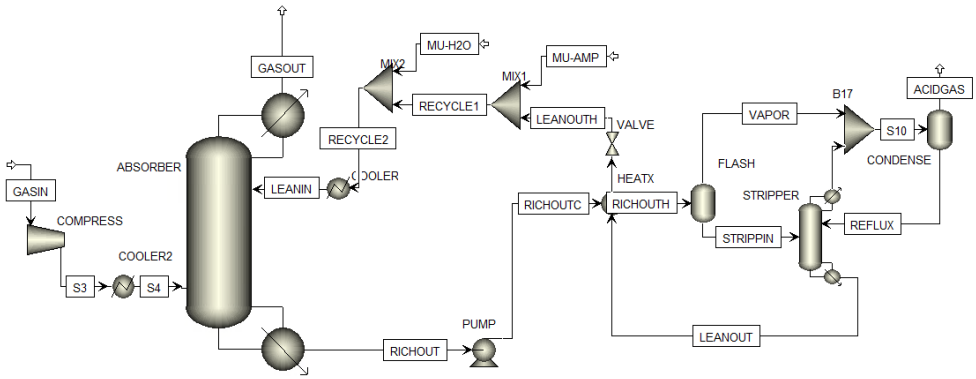

Figure 6.7: A screen shot of the process flow diagram from Aspen Plus for the flue gas compression modification.

.

The variations made on the feed gas compression modification are shown in Table 6.5. Two pressures was evaluated, with and without cooling of the compressed gas.

Table 6.5: Variations on feed gas compression

	Pressure[bar]	
With cooling	2	3
Without cooling	2	3

6.3.4 Lean Vapor Compression Setup

A flash tank was inserted to the lean solvent stream leaving the stripper bottom. The operation pressure and duty were specified for the flash tank. The duty was kept constant at zero. The rich gas stream leaving the flash tank was re-compressed to the stripper pressure. For the 0.5 [bar] flash tank, the rich solvent was pressurises to the absorber pressure. The variations can bee seen in Table 6.6. Figure 6.8 shows the setup in Aspen Plus.

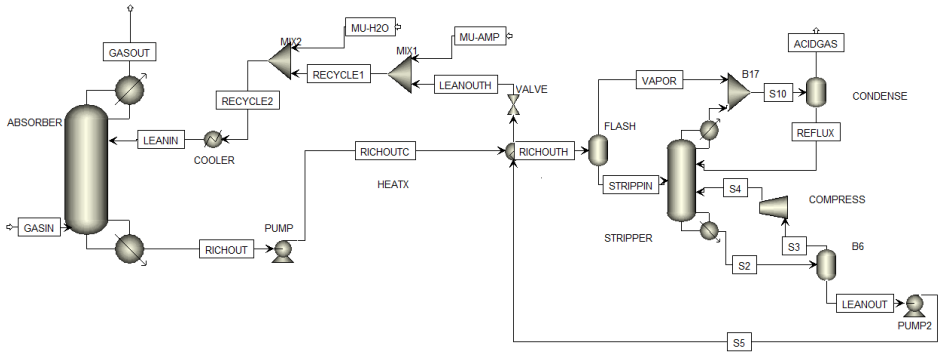

Figure 6.8: A screen shot of the process flow diagram from Aspen Plus lean vapor compression modification.

.

6.3.5 Rich Vapor Compression Setup

The modification in Aspen Plus involved redirecting the vapor stream from the flash before the stripper. The rich vapor stream was compressed and sent to the bottom of the stripper column. The Rich solvent stream was sent to a pump to elevate the pressure to that of the stripper. A second heat exchanger was inserted to increase the rich solvent after the temperature decrease in the flash tank The rich solvent was heat exchanged with the hot lean solvent out of the stripper column, prior to the primary heat exchanger. The second heat exchanger was design with a temperature difference of 8 [°C], between the hot inlet and the cold outlet. The duty in the flash tank was kept constant at zero, and the pressure of the flash tank was variated according to Table 6.6. Figure 6.9 shows the setup in Aspen Plus.

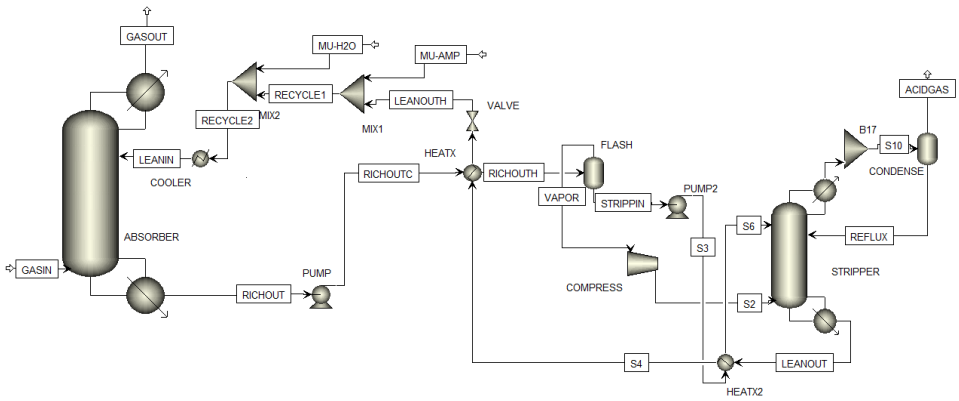

Figure 6.9: A screen shot of the process flow diagram from Aspen Plus rich vapor compression modification.

.

The variations can be seen in Table 6.6.

Table 6.6: Variations on Lean and rich vapor compression

	Flash pressure[bar]		
LVC	1.5	1.0	0.5
RVC	1.6	1.3	1.0

6.3.6 Rich Solvent Split Setup

A splitter was inserted on the rich solvent outlet before the primary heat exchanger. The smaller fraction was sent to a heat exchanger on the stripper outlet stream. The second heat exchanger was designed as the first, with a temperature difference of 8 [°C] between the hot outlet stream and the cold outlet stream. It was experienced that the primary heat exchanger was operating beyond the pinch point for the 0.8 and 0.7 split fraction, as a result of the heat recovered in the secondary heat exchanger. Alterations were made on the specifications to 12 and 16 [°C] temperature difference between the hot inlet and the cold outlet for the 0.8 and 0.7 split fractions accordingly, to achieve the same pinch as for the 0.9 split fraction. The colder and smaller fraction of the rich solvent was fed to the higher stages of the stripper, and the hot primary feed on a lower stage. This is stated in Table 6.7. The parameter variation was similar to the ICA and RSR modifications. One parameter was changed at a time, and two others held constant. THe constant values are given in bold in Table 6.7. Figure 6.10 shows the setup in Aspen Plus.

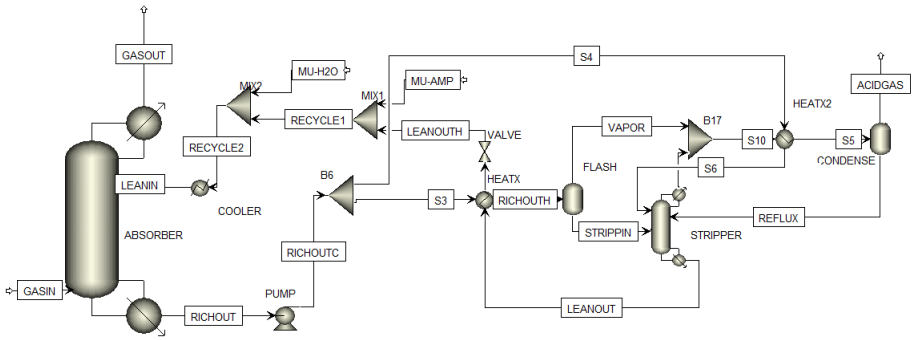

Figure 6.10: A screen shot of the process flow diagram from Aspen Plus for the rich solvent splitting modification.

.

Table 6.7: Variations made for the rich solvent split modification. The numbers given i bold were the values for the two variables kept constant, while the other parameter was changed.

Top feed stage from top	**1**	3	5
Lower feed stage from top	**6**	4	2
Split fraction	**0.1**	0.2	0.3

6.3.7 Summary of Modification Variables

Table 6.8 shows all the changed parameters and their values, used in evaluating the process modifications.

Table 6.8: This tables shows a summary of all the variables used for the process modification.

Parameters	**Variables**		
	1	**2**	**3**
ICA[a]			
Feed stage	9	15	
Cooling temperature [°C]	10	40	
Split fraction	0.1	0.3	
RSR[b]			
Feed stage	9	15	
Cooling temperature [°C]	10	40	
Split fraction	0.1	0.3	
FGC			
Pressure (without cooling) [bar]	2	3	
Pressure (with cooling) [bar]	2	3	
LVC			
Flash pressure [bar]	1.5	1	0.5
RVC			
Flash pressure [bar]	1.6	1.3	1
RSS[c]			
Feed stage (Upper)	3	5	
Feed stage (Lower)	4	2	
Split fraction	0.2	0.3	

[a] Constant values: Feed stage, 12. Temperature, 25 [°C]. Split fraction, 0.2

[b] Constant values: Feed stage, 12. Temperature, 25 [°C]. Split fraction, 0.2

[a] Constant values: Feed stage (upper), 1. Feed stage (lower), 6. Split fraction, 0.2

Chapter 7

Process Modifications Simulation Results

7.1 Base Case

7.1.1 Simulation Results

The results from the simulation of the base case can be viewed in Table 7.1.

From table 7.1 the operation characteristics of the base case is shown. In regards to the heat loss, it can be seen that a majority of the heat is reclaimed in the heat exchanger. From the required cooling in the condenser and the cooler it can be seen that the system has potential for improvement and reduced heat loss. It should also be noted that the utilized potential of the AMP is quite low, seen in Table 7.1 as the low cyclic loading, this is a result of the high solvent flow rate.

7.1.2 Discussion

The liquid to vapor flow ratio was high compared to typical flue gas CO_2 absorption with amines. A study by [59] for biogas upgrading with same conditions as this study, used a liquid to vapor ratio of approximately 7 using 50[wt%] MDEA. Similar for flue gas cleaning [60] using AMP. A possible explanation for the high solvent flow rate was that the temperature in the absorption column became to too high with low solvent flow rate, seen in Figure 6.4. At 40 [°C] and 0.3 loading, AMP has approximately 30% higher heat of absorption compared to MDEA [26]. It can be seen that the temperature in the column increases abruptly to around 80 [°C] for the solvent loading of 6 [kmol/h]. The large concentration of CO_2 in biogas and available AMP reacts, the heat of reaction accumulates and makes the

Table 7.1: Base case simulation results

Pump		24
Reboiler		7866
Heat exchanger		12787
Condenser	[W]	-2329
Cooler		-5223
Equivalent electricity(Karimi et al.[34])		1204
Equivalent electricity [53]		3957
Q_R/CO_2	[kJ/kgCO_2]	3416
W_{eq}(Karimi et al.[34])	[kJ/kgCO_2]	523
W_{eq} [53]	[kJ/kgCO_2]	1718
Lean load		0.300
Rich load	[α]	0.561
Cyclic load		0.260
Solvent flow	[kmol/h]	11
Rich out absorber		53
Rich in stripper(top)	[°C]	99
Lean out stripper(btm)		110

temperature increase. After the temperature reaches 80 [°C] the high temperature limits the exothermic reaction, thus limits the amine from further reaction. For higher solvent loadings more mass is available to absorb the reaction heat, thus limiting the temperature increase. From Figure 6.4 it can be seen that the absorption and temperature increase is much smoother. Based on the above it was assumed that temperature increase in the absorption column became a limiting factor. Resulting in lower rich loadings achievable. In order to achieve the same cyclic loading and CO_2 removal, lean loadings needed to be lowered to compensate for the reduced rich loading. This increased the heat demand in the stripper. The temperature bulge seen in Figure 6.4 gives an indication on possible placement for intercooling.

The specific desorption heat for 30[wt%] AMP with 5[wt%] Pz was reported by [61] to 3870 [kJ/kg CO_2]. From the literature survey in their report, they found a typical value for the reboiler duty for flue gas CO_2 capture to approximately 3750 [kJ/kgCO_2]. The value found for the base case in this study was 3416 [kJ/kgCO_2], which was considered to be in reasonable agreement. The specific heat demand was expected to be lower than for flue gas capture. The reason for this is twofold. As noted in Section 5.5, the heat loss in the stripper column was not accounted for, due to low desorption rates for the simulated model compared to the experimental

pilot. Secondly, the concentration of CO_2 is typically around 10% in flue gas versus 40% for biogas, resulting in higher CO_2 partial pressure in biogas. The increased partial pressure causes a larger driving force in the absorption column, hence higher loadings, and less heat demand in the stripper.

7.2 Intercooled Absorber

7.2.1 Simulation Results

The results of the intercooled absorber is shown in Table 7.2.

Table 7.2: Results for the intercooled absorber modification

		Base	Split fraction			Cooling temp		Feed stage		Optimal		
		case	0.1	0.2	0.3	10	40	9	15	I	II	II
Pump		24	26	25	25	24	24	25	25	24	18	9
Reboiler		7866	7694	7618	7545	7447	7691	7582	7624	7370	6965	6356
Heat exchanger		12787	13547	13786	14013	14007	13103	12919	13612	14944	11398	8017
Condenser	[W]	-2329	-2134	-2116	-2100	-2080	-2212	-2115	-2117	-2076	-2067	-2334
Cooler		-5223	-4739	-4270	-3830	-3463	-4674	-4012	-4410	-2489	-2313	7
Cooling(2)			-520	-932	-1311	-1595	-496	-1153	-796	-2496	-2268	-3444
Equivalent electricity		3957	3873	3834	3797.5	3747.5	3869.5	3816	3837	3709	3500.5	3187
W_{eq}[kJ/kgCO_2]		1718	1682	1665	1649	1627	1680	1657	1666	1611	1520	1384
W_{eq} reduction			2.1%	3.1%	4.0%	5.3%	2.2%	3.6%	3.0%	6.3%	11.5%	19.5%
Q_R/CO_2[kJ/kgCO_2]		3415	3341	3308	3276	3234	3340	3293	3311	3200	3025	2760
Reboiler reduction			2.2%	3.2%	4.1%	5.3%	2.2%	3.6%	3.1%	6.3%	11.5%	19.2%
Lean load		0.300	0.3179	0.3278	0.3332	0.335	0.316	0.3259	0.3278	0.337	0.264	0.055
Rich load	[α]	0.561	0.5783	0.5882	0.5936	0.596	0.576	0.5863	0.5882	0.598	0.559	0.646
Cyclic capacity		0.260	0.260	0.260	0.260	0.261	0.260	0.260	0.260	0.260	0.295	0.591
Solvent flow	[kmol/h]	11.0	11.0	11.0	11.0	11.0	11.0	11.0	11.0	11.0	8.0	4.0
Temperatures												
Rich out absorber		53	50	48	47	46	51	49	48	44	44	31
Rich in stripper(top)	[°C]	99	99	98	98	98	99	98	99	97	98	100
Lean out stripper(btm)		110	110	109	109	109	110	109	110	109	111	120

It was found that the intercooling had a major impact on the absorption column. As seen in Table 7.2, the intercooled setup which gave the most reduction was with; split fraction, 0.3, cooling temperature, 10 [°C], and cooling stage, 9. This was used in three optimized cases to further study the impact on the system. I) Constant solvent flow rate, equal to base case, 11 [kmol/h], II) Reduced solvent flow rate according to red line in Figure 7.1, with constant split fraction of 0.7, III) Reduced solvent flow rate with a constant flow to intercooling of 3.3 [kmol/h], i.e. increasing split fraction with reduced solvent flow rate, according to blue line in Figure 7.1.

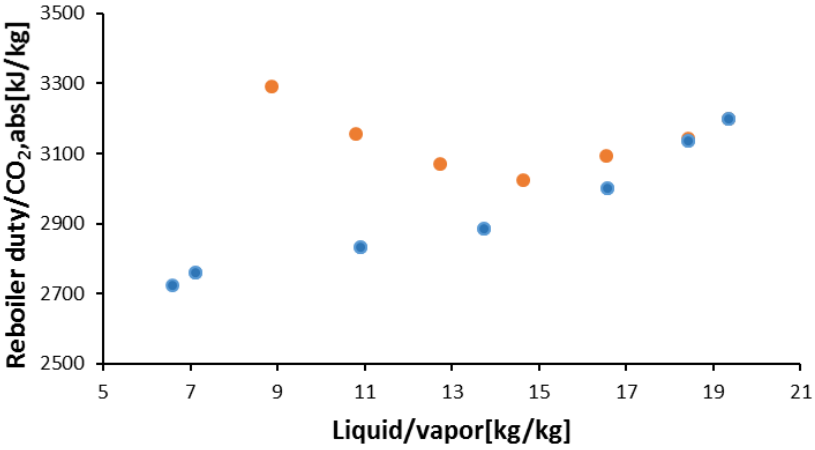

Figure 7.1: Liquid to gas ratio versus the specific reboiler duty. Orange line showing the constant split fraction of 0.3. The blue line showing increased split fraction.

.

Temperature profiles for various cases for the intercooled absorber can be seen in Figure 7.2.

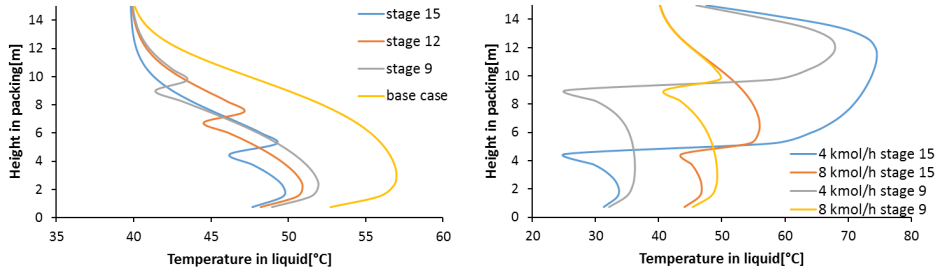

(a) (b)

Figure 7.2: The temperature profile in the absorption column for various cooling stages options compared to the base case. Figure a) shows the temperature distribution as a result of cooling stage, Figure b) shows the temperature profiles for the optimum cases I) and II), and with cooling on stage 15.

7.2.2 Discussion

From the reduced duty of the condenser and cooler in Table 7.2, it can be seen that the intercooling reduced the heat loss from the system. The reduced temperature in the absorption column reduced the the temperature of the rich solvent stream out. This increased the potential of this stream to absorb heat in the heat exchanger, which again reduced the temperature of the lean solvent out of the heat exchanger causing less cooling on this stream pre entering the absorption column. A small reduction in the reboiler was also experienced. From Table 7.2 and Figure 7.1 it can be seen that large reduction in the solvent loading can be achieved by introducing intercooling, and the cyclic loading increases.

The intercooling lead to a significant reduction in required solvent flow rate. It can be seen from Figure 7.1 that by increasing the cooling, less solvent was needed. The trend in Figure 7.1 indicates even lower solvent to gas rates for increased split fraction. Further reductions were not achieved, because of limitations in the simulation model. The reduction in required solvent can be explained by improved absorber kinetics by reduced temperature. Hence making it possible to utilize more of the loading potential of the solvent seen by increased cyclic loading.

With regard to the options for optimal intercooling, it was found that the largest amount of cooling resulted in the largest energy reduction. It was found that intercooling on stage 9 lead to the largest energy reduction. From Figure 7.2(a) it can be seen that, cooling smooths the temperature increase, even though the temperature of the rich solvent out is largest. The high temperatures seen in Figure 7.2(b) indicate a possibility for increased energy reduction by several intercooling stages, mentioned by [32]. Figure 7.2(b) also indicates that the intensity of the cooling for the solvent flow of 4 [kmol/h] might be to high, as the temperature is less than 40 [°C] for the lower parts of the column. This also indicates that several cooling stages could be advantageous.

For the constant solvent loading of 11 [kmol/h] it was found that a 6.3% reduction for the reboiler duty and the overall energy requirement was possible, compared to the base case. Experimental results performed on flue gas capture with 30[wt%] AMP + Pz, by Knudsen et. al [35] reported a 7% reduction in regeneration energy, which indicates that the values are reasonable.

7.3 Rich Solvent Recycle

7.3.1 Simulation Results

Table 7.3: Results for the rich solvent recycle modification

		Base case	Feed stage 9	Feed stage 12	Feed stage 15	Cooling temp 10	Cooling temp 40	Split fraction 0.1	Split fraction 0.3	Opt I	Opt II
Pump		24	24	24	24	24	24	24	23	23	15
Reboiler		7866	7532	7509	7523	7392	7676	7654	7395	7247	7007
Heat exchanger		12787	13826	13591	13611	14165	13056	13149	14078	14983	9729
Condenser	[W]	-2329	-2114	-2140	-2151	-2086	-2238	-2202	-2107	-2053	-2268
Cooler		-5223	-3838	-3797	-3798	-3090	-4526	-4504	-3097	-2044	-2293
Cooler(2)			-1272	-1258	-1259	-1902	-595	-633	-1874	-2836	-2105
Equivalent electricity		3957	3790	3778.5	3785.5	3720	3862	3851	3720.5	3646.5	3518.5
W_{eq}[kJ/kgCO_2]		1718	1646	1641	1644	1615	1677	1672	1616	1584	1528
W_{eq} reduction			4.2%	4.5%	4.3%	6.0%	2.4%	2.7%	6.0%	7.8%	11.1%
Q_R/CO_2[kJ/kgCO_2]		3415	3271	3261	3267	3210	3333	3324	3211	3147	3043
Reboiler reduction			4.2%	4.5%	4.4%	6.0%	2.4%	2.7%	6.0%	7.9%	10.9%
Lean load		0.300	0.335	0.335	0.334	0.344	0.321	0.321	0.346	0.357	0.1911
Rich load	[α]	0.561	0.625	0.625	0.624	0.634	0.613	0.593	0.659	0.670	0.5199
Cyclic capacity		0.260	0.290	0.290	0.290	0.290	0.292	0.272	0.313	0.313	0.329
Solvent flow	[kmol/h]	11.0	11.0	11.0	11.0	11.0	11.0	11.0	11.0	11.0	6.5
Temperatures											
Rich out absorber		53	47	47	47	44	50	50	45	40	46
Rich in stripper(top)	[°C]	99	98	98	98	98	99	99	98	97	100
Lean out stripper(btm)		110	109	109	109	109	110	110	109	108	115

The feed stage of the cooling however, was found to be optimal for stage 12, unlike ICA with optimum at stage 9. The best setup was used in the optimum cases I) and II). The L/G vs reboiler duty diagram is shown in Figure E.1 in Appendix E. The the results for the rich solvent recycle is shown in Table 7.3.

7.3.2 Discussion

As expected the ICA and RSR had similar impacts on the system. From Table 7.3 it can be seen that the major difference between the two, is the enhanced absorption capacity seen as the increased rich loading for the RSR modification. The rich loading was increased for larger split fraction, as a result of more solvent sent in recycle, hence increasing the contact time between the solvent and the gas. The cooling had similar effect on the absorption column as for the ICA. Not quite expected, was the effect on the feed stage, where it was found that stage 12 was the most effective, unlike the ICA with a higher feed stage of 9. This might be a result of the recycled solvent, already being rich in CO_2, hence the solvent being less reactive. The cyclic loading was found to increase for the RSR, even though the amount of absorbed CO_2 in the system was held constant. The difference in cyclic loading was a assumed to be a result of less CO_2 dissolved in the water

phase, as the calculation of loading is limited to the CO_2 and AMP species.

The reboiler duty was reduced by 8.1% compared to the base case, which was a bit higher than the ICA. It was found that even less solvent could be used for RSR compared to the ICA, with optimal solvent flow rates of 6.5 [kmol/h] and 8.0 [kmol/h] respectively. This reduction can be explained as a result of the increased contact time and loading by implementing RSR.

7.4 Feed Gas Compression

7.4.1 Results

The results of the FCE modification can be viewed in Table 7.4.

Table 7.4: Results for the feed gas compression modification

Pressure	[bar]	Base case	With cooling 2	With cooling 3	Without cooling 2	Without cooling 3	Opt
Pump		24	0	0	0	0	
Pump(2)			0	23	0	23	20
Reboiler		7866	6947	6631	6986	6709	6593
Heat exchanger		12787	10849	10066	10624	9638	8532
Condenser	[W]	-2329	-1584	-1369	-1597	-1394	-1476
Cooler		-5223	-5267	-5229	-5542	-5764	-5080
Cooler(2)			-250	-482	0	0	-482
Compressor			347	576	347	576	482
Equivalent electricity		3957	3820.5	3891.5	3840	3930.5	3778.5
W_{eq}[kJ/kgCO_2]		1718	1659	1690	1668	1707	1641
W_{eq} reduction			3.4%	1.7%	3.0%	0.7%	4.5%
Q_R/CO_2[kJ/kgCO_2]		3416	3017	2880	3034	2913	2863
Reboiler reduction			11.7%	15.7%	11.2%	14.7%	16.2%
COF compressor			2.65	2.14	2.54	2.01	2.64
Lean load		0.300	0.420	0.477	0.417	0.470	0.385
Rich load	[α]	0.561	0.712	0.804	0.709	0.797	0.695
Cyclic capacity		0.260	0.292	0.326	0.292	0.326	0.309
Solvent flow	[kmol/h]	11.0	11.0	11.0	11.0	11.0	9.0
Temperatures							
Gas out compressor			88	129	88	129	129
Rich out absorber	[°C]	53	54	54	55	60	57
Rich in stripper(top)			93	90	93	94	92
Lean out stripper(btm)		110	105	103	105	108	106

The optimum was decided as the most reduction in reboiler duty. The optimum case was found to be feed gas compression to 3 [bar] with cooling. The flow rate for the optimum was reduced to 9 [kmol/h]. The L/G vs reboiler duty diagram is shown in Figure E.1 in Appendix E.

7.4.2 Discussion

From Table 7.4 it can be seen that the compression of feed gas results in higher loadings, as the driving force in the absorption column was increased. The increased loading also lead to higher temperatures of the rich solvent out of the absorber. This in turn reduced the duty of the heat exchanger as the temperature difference was decreased.

Interestingly the largest reduction in the reboiler duty was found by compressing the feed gas to 3 [bar]. The calculated equivalent energy reduction on the other hand was largest for lower compression to only 2 [bar]. The coefficient of performance (COP) gives the coefficient for reduced heat energy in the reboiler divided by invested mechanical energy in the compressor. It is important to remember the selected method for calculating the equivalent electricity for steam demand in the reboiler, and how this method, as well as the cost of energy, influences the result.

The cooling of the gas after compression accounts for 1% of the energy reduction. The temperature of the compressed gas was 129 [°C]. For the cases with cooling the gas temperature was reduced to 40 [°C], before injection to the column. It may therefore be argued that the energy consumption of the system is relatively insensitive to the temperature of the inlet gas stream.

From Figure E.1 it can be seen that the modification has little effect on the solvent flow rate. This indicates that the system is dependent on cooling in the absorption column, in order reduce solvent flow. The purpose of the feed gas compression modification is to increase the driving force, thus increase the rich loading achievable. This in turn reduces the solvent flow rate, which reduces the reboiler duty. However the reduction in solvent flow was found to be optimal at 9 [kmol/h], this is a modest reduction compared to ICA and RSR. This indicates that the required cooling in the absorption column is a limiting factor in the system.

7.5 Lean Vapor Compression

7.5.1 Simulation Results

Table 7.5: Results for the lean vapor compression modification

		Base case	Flash pressure [bar] 1.5	1	0.5	Opt
Pump		24	24	23	23	17
Reboiler		7866	7422	6717	5322	5235
Heat exchanger		12787	10957	8332	4282	2535
Condenser	[W]	-2329	-1934	-1460	-833	-1117
Cooler		-5223	-5204	-5149	-5149	-4754
Compressor			33	213	970	1005
Pump(2)			0	0	12	8
Equivalent electricity		3957	3768	3594.5	3654	3639.5
W_{eq}[kJ/kgCO_2]		1718	1636	1561	1587	1580
W_{eq} reduction			4.78%	9.16%	7.66%	8.02%
Q_R/CO_2[kJ/kgCO_2]		3416	3223	2917	2311	2273
Reboiler reduction			5.64%	14.61%	32.34%	33.45%
COF compressor			13.5	5.4	2.6	2.6
Lean load		0.300	0.301	0.294	0.294	0.109
Rich load	[α]	0.561	0.534	0.644	0.644	0.410
Cyclic capacity		0.260	0.233	0.350	0.350	0.302
Solvent flow	[kmol/h]	11.0	11.0	11.0	11.0	7.0
Compressed gas	[kg/h]		2.37	5.70	11.7	10.7
Temperatures						
Rich out absorber		53	53	53	53	59
Rich in stripper(top)	[°C]	99	96	89	72	75
Lean out stripper(btm)		110	109	108	105	117

The optimum was based on largest reduction in reboiler duty. This was found for a flash pressure of 0.5 [bar], seen in Table 7.5. For the optimum case, the solvent flow rate was reduced to 7.0 [kmol/h]. The L/G vs reboiler duty diagram is shown in Figure E.1 in Appendix E

7.5.2 Discussion

According to Table 7.5 the LVC displays good reductions for both reboiler duty and energy requirement. The lean solvent leaving the flash tank has reduced temperatures compared to the base case, this can be seen in the reduction in the heat exchanger duty. Furthermore this reduces the rich solvent inlet to the stripper column, seen in Table 7.5 and lowers the temperature in the top of the stripper which again reduces the heat loss in the condenser. Interestingly, the reduction in heat exchanger duty, does not increase the cooling of the lean solvent feed to the absorption column. Similar to the FGC modification, the largest reduction in reboiler duty was not the most energy efficient setup, calculated here.

The COF for the LVC is more than twice as large as for the FGC. Larger reductions in solvent flow rate is also possible with the LVC, seen in Figure E.1.

According to [32] large reductions can be expected of LVC modification, they stated from 1.4% to 11.6% parasitic reduction for flue gas capture. A simulation study with the specialized CO_2 capture simulator CO2SIM presented by [62], found a 13% reduction in reboiler duty with 30[wt%] AMP+Pz for atmospheric flash LVC. This is in good agreement with the 14.6% found in this study.

7.6 Rich Vapor Compression

7.6.1 Simulation Results

Table 7.6: Results for rich vapor compression modification

Flash pressure	**[bar]**	**Base case**	**1.6**	**1.3**	**1.0**
Pump		24	15	7	0
Reboiler		7866	7835	7817	7801
Heat exchanger		12787	10318	9204	7791
Condenser		-2329	-2302	-2299	-2297
Cooler	[W]	-5223	-5230	-5225	-5218
Heat exchanger(2)			2560	3679	5090
Comp			10	18	25
Pump(2)			10	18	27
Equivalent electricity		3957	3952.5	3951.5	3952.5
W_{eq}[kJ/kgCO_2]		1718	1716	1716	1716
W_{eq} reduction			0.11%	0.14%	0.11%
Q_R/CO_2[kJ/kgCO_2]		3415	3402	3261	3266
Reboiler reduction			0.39%	0.62%	0.83%
COF compressor			0.012	0.013	0.013
Lean load		0.300	0.298	0.298	0.298
Rich load	[α]	0.561	0.544	0.544	0.544
Cyclic capacity		0.260	0.246	0.246	0.246
Solvent flow	[kmol/h]	11.0	11.0	11.0	11.0
Compressed gas	[kg/h]		1.12	1.13	0.99
Temperatures					
Rich out absorber		53	53	53	53
Rich in stripper(upper)	[°C]		99	99	99
Rich in stripper(lower)		99	118	138	163
Lean out stripper(btm)		110	110	108	105

It was not found any benefits of reducing the solvent flow. Hence no optimized solution is shown. The L/G vs reboiler duty diagram is shown in Figure E.1 in Appendix E. The simulation results for the RVC can be seen in Table 7.6.

7.6.2 Discussion

The RVC modification had minimal beneficial effect on the system. A reduction in reboiler duty less than 1% was found, and even less reduction in energy demand when counting the energy consumption in the compressor and additional pump. One reason why this modification had minimal effect might be that the flashing of the rich solvent was already installed for the base case. As a result the benefits are seen are a result of the gas compression and the additional heat exchanger and reduced flash tank pressure. The additional heat exchanger did not reduce the heat loss in the system. This can be seen from the relative constant value for the condenser and the cooler compared to the base case.

There are several reasons for the difference in modification effect for the LVC and RVC. Firstly, the compressed gaseous stream has high CO_2 content for the RVC and low content for the LVC. For the RVC it might be more efficient to send the gasous stream directly to the condenser, instead of sending the CO_2 rich stream to the bottom of the stripper. Secondly, the temperature of the stream into the flash tank is much higher for the LVC than the RVC. This results in a larger hot compressed stream injected to the bottom of the stripper.

7.7 Rich Solvent Split

7.7.1 Results

Table 7.7: Results from the rich solvent splitting modification

		Base case	Top stage feed 1	Top stage feed 3	Top stage feed 5	Split fraction 0.8	Split fraction 0.7	Btm stage feed 2	Btm stage feed 4	Opt
Pump		24	25	25	25	25	25	25	25	25
Reboiler		7866	6600	6617	6646	7086	8120	6826	6657	6600
Heat exchanger		12787	13099	13099	13100	12062	11021	13099	13099	13099
Condenser	[W]	-2329	-1002	-1019	-1049	-454	-445	-1229	-1060	-1002
Cooler		-5223	-5293	-5293	-5293	-6332	-7375	-5293	-5294	-5293
Heat exchanger(2)			877	860	1070	1151	1034	930	892	877
Equivalent electricity		3957	3325	3334	3348	3568	4085	3438	3354	3325
W_{eq}[kJ/kgCO_2]		1718	1444	1448	1454	1549	1774	1493	1456	1444
W_{eq} reduction			16.0%	15.8%	15.4%	9.8%	-3.2%	13.1%	15.3%	16.0%
Q_R/CO_2[kJ/kgCO_2]		3416	2866	2873	2886	3077	3526	2964	2891	2866
Reboiler reduction			16.1%	15.9%	15.5%	9.9%	-3.2%	13.2%	15.4%	16.1%
Lean load		0.300	0.313	0.307	0.308	0.307	0.317	0.335	0.328	0.337
Rich load	[α]	0.561	0.540	0.525	0.530	0.525	0.548	0.596	0.589	0.598
Cyclic capacity		0.260	0.227	0.218	0.221	0.218	0.231	0.261	0.261	0.260
Solvent flow	[kmol/h]	11.0	11.0	11.0	11.0	11.0	11.0	11.0	11.0	11.0
Temperatures										
Rich out absorber		53	52	52	52	52	52	52	52	52
Rich in stripper(top)	[°C]	99	88	88	89	76	67	90	89	89
Rich in stripper(lower)			101	101	101	102	103	101	101	101
Lean out stripper(btm)		110	110	110	110	110	110	110	110	110

It was initially found that the most beneficial split fraction was the lowest with 0.9. This was used for the testing of optimal stage for the top and lower stripper feeds. The most effective alterations for the RSS modification were found as: **a)** Split fraction, 0.9 **b)** Feed stage top: 1 **c)** Feed stage lower: 6

These were applied in the optimized solution seen in Table 7.7. It was not found beneficial to further reduce the solvent flow in regards to the reboiler duty, seen in Figure E.1 in Appendix E.

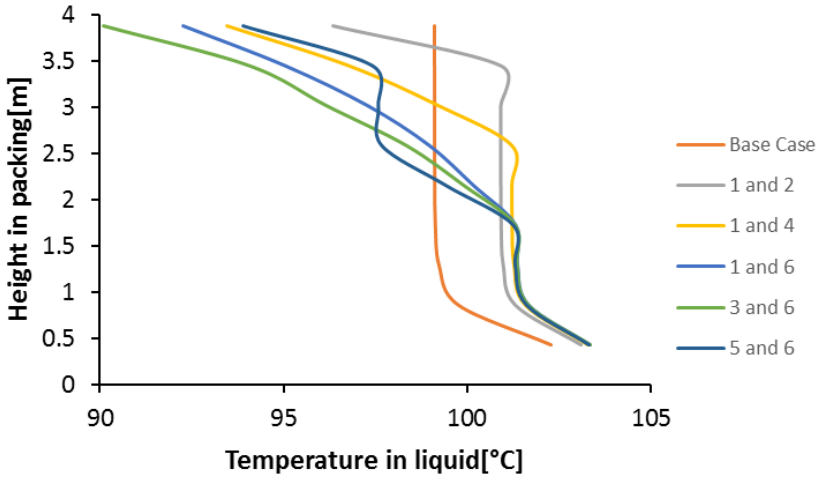

Figure 7.3: Temperature profiles for the stripper with different top and lower rich solvent feed stages, given in the legend as the first and second number receptively.

7.7.2 Discussion

From Table 7.7 it can be seen that the RSS made large reductions to the reboiler duty and equal reduction in the total energy consumption. The optimal split fraction was found to be 0.9. It can be seen from Table 7.7 that the increased split fraction reduced the primary heat exchanger duty, since the solvent flow was reduced. For the secondary heat exchanger on the other hand, the maximum heat transfer was found for a split fraction of 0.8, however the duty in the primary heat exchanger was far greater than for the secondary. A split fraction of 0.9 has the largest combine heat exchanger duty. It can be seen from the reduced condenser duty that the RSS successfully increases the heat integration of the system. The reduction in the condenser can be seen as a relative reduction in the reboiler duty. It is interesting to notice that a split fraction of 0.7 has a negative effect on the system.

It was found that the optimal feed stages were 1 and 6. This was assumed to correspond to the most efficient temperature gradient in the column. From Figure 7.3 it can be seen that the lower feed stage with most potential had neither the highest or the lowest temperature in the top of the stripper, but the optimal was found in between with stages 1 and 6. The temperatures stated for the RSS in Table 7.7, show that the modification successfully reduces the temperature in the stripper top. Hence reducing the heat loss from the system. This can be seen directly from the reduced condenser duty.

The reduction in energy requirement when implementing RSS is a direct result of minimizing the heat loss in the gas out of the stripper.

7.8 Results Summary

Table 7.8: Results for the optimised process modifications reviewed

Modifications	Reboiler duty [W]	Reboiler duty Reduction	W_{eq} [kJ/kgCO_2]	W_{eq} Reduction	Solvent flow rate[kmol/h]	Flow rate reduction	Cyclic [α]	Loading change
Base case	7866		1718		11		0.260	
ICA	6965	11.5%	1520	11.5%	8	27.3%	0.295	13.2%
ICA(reduced solvent)	6356	19.2%	1384	19.5%	4	63.6%	0.591	127.0%
RSR	7007	10.9%	1528	11.1%	6.5	40.9%	0.329	26.3%
LVC	5235	33.4%	1580	8.0%	7	36.4%	0.302	15.8%
RVC	7801	0.8%	1716	0.1%	11	0.0%	0.246	-5.5%
FGC	6593	16.2%	1650	4.0%	9	18.2%	0.309	18.7%
RSS	6600	16.1%	1444	16.0%	11	0.0%	0.260	0.0%

Table 7.8 displays the optimized cases for the process modifications, with the optimal flow rate. The reduction in reboiler duty is given as well as the reduction in equivalent electricity.

Technical values stated for commercial chemical absorption biogas upgrading plants [7] are compared to some of the cases in this study and shown in Table 7.9

Table 7.9: Values stated by manufacturers of chemical absorption plants for biogas upgrading [7] and the some of the cases included in this study.

		[7]	Base case	LVC	RSS
Electricity required	[kWh/Nm3]	0.140	0.002	0.086	0.002
Heat required	[kWh/Nm3]	0.55	0.79	0.44	0.55
Methane slip	[%]	0.060	0.015	0.009	0.014
Chemicals carry-over	[kg/Nm3]	3.0E-05[a]	2.3E-07	4.82E-07	2.38E-07

[a] Including anti-foam, amine make-up, etc.

7.9 Discussion

From Table 7.8 it can be seen that most of the process modifications, with the exception of the RVC, causes significant reductions in the energy demand for the process. **a)** Largest reboiler reduction: LVC, **b)** Largest equivalent electricity reduction: ICA, and **c)** Largest solvent reduction: ICA

The findings from studying the base case and the effect of intercooling suggests that there is a large need for cooling in the absorption column when AMP is applied as solvent for biogas capture, due to the exothermic nature of the absorption reaction. Compared to processes with flue gas this is an important difference as

the partial pressure of CO_2 in the biogas typically can be significantly higher than for flue gas systems, both due to concentration and absolute pressure. It was found that high solvent flow rates could reduce the temperature increase by acting as a cooling medium, stabilizing the temperature in the absorption column. It was later experienced that the solvent flow rate could be drastically reduced when cooling was introduced in the absorption column. This identifies an issue related to chemical absorption of CO_2 from high concentrations in biogas, when amines with high reaction heat are applied, and that cooling is required for efficient operation. The findings in this study suggest that more cooling is needed than applied here, and a potential for increased benefits with several cooling stages.

The largest reduction in reboiler duty was found for the LVC, with a 33.4% reduction. However the reduction comes at the cost of mechanical work needed in order to operate the compressor. As a result the calculated equivalent electricity reduction was 8.0%, which is still significant. The largest equivalent electricity reduction was found for the RSS modification with a 16.0% reduction. This was mostly a result of reducing the heat loss from the system, which directly related to reduction in the reboiler duty. This modification did, however, not reduce the optimal solvent flow. The factor used for converting reboiler heat to equivalent electricity was in this report given as 0.5. Other studies such as [33] uses lower factors. This increases the importance of additional mechanical work relative to the heat demand in the reboiler. The converting factor needs to be evaluated for each plant and case, as it has a large impact on relative effect of each modification.

The results found in this chapter for the base case and the process modifications should be viewed in the context of the findings in Chapter 5.2 and Chapter 5.5. For higher loadings it was found that the absorption rate was underestimated for the simulation model compared to experimental data, and a general underestimation of the desorption. It can therefore be argued, that a real system may perform better than the results of this simulation model.

The complexity and cost of implementation was identified in the literature survey as important factors for implementation of process modifications. The ICA and RSR are arguably the implementations which imposes the least increase in complexity and additional cost. The RSS requires an additional heat exchanger. The other cases adds more equipment and more input energy. Increased complexity of the process will in many cases increase the additional process equipment needed. The viability of the investment will vary for large coal plant carbon capture plants and small scale biogas upgrading plants. It can be argued that for smaller scale operations such as biogas upgrading plants, the complexity and additional equipment are just as, or more important factors, than for larger scale flue gas capture plants.

The modifications are based on an assumption of access to and abundant cheap cool water or air, which is considered possible for operation in the cool climate of the Nordic countries, although cost of cooling is generally dependent on local conditions [54]. Karimi et al. [34] stated "Cooling below 30 [°C] in industry is normally not easy and cheap and was therefore not investigated", without further justification. The required energy for cooling has not been evaluated, as this was deemed negligible in comparison to the heat demand in the reboiler and compressor work.

From Table 7.9 some of the cases simulated in this study has been compared to values stated by manufacturers of chemical biogas upgrading plants for biogas. It can be seen that the electricity required for operation is far less than stated for actual plants. This implies that in order to establish a simulation of a full scale plant, a more comprehensive model is needed. The heat demand is more comparable, since the heat demand is mainly limited to the reboiler duty. It can be seen that the base case does not appear to be competitive against commercially available plants. When implementing modifications on the other hand, it can be seen that for the LVC modification, the heat demand is reduced by 20% compared to actual plants. A bit unexpected was the low carry-over compared to that of the commercially available plants, since MDEA is most widely used amine for chemical absorption of CO_2 form biogas, and AMP has higher volatility than MDEA. This might partly be a result of no added chemicals (such as anti-foaming etc.) in addition to AMP. The low methane slip suggest favourable conditions when AMP is applied.

Chapter 8

Conclusion

In this Master's Thesis, an Aspen Plus simulation model has been developed and compared to experimental data. Both VLE and pilot validations have been performed. It was found that simulation results best matched the VLE data for lower concentrations and temperatures in the range 40-100 [°C]. The validation of the absorption and desorption revealed that the simulation model had a tendency to underestimate the absorption rate for larger loadings, and a general underestimation of the desorption rate. As a result it might be argued that a biogas plant based on the configuration(s) studied in this thesis might perform better than the predictions of the simulation model. The AAD for the absorption column validations was found to 12.8% and 8.0% for the desorption column. The simulation model predicted temperature profiles for the absorption and desorption column in good agreement with experiments.

Possible process improvements have been evaluated using the simulation model developed as part of this work. These process modifications reveal a significant potential for improvement for chemical absorption processes when AMP is applied. All evaluated process modifications, with the exception of RVC, increased the efficiency of the process. It was found that large reductions could be made, with relatively simple alterations to the conventional process design.

The evaluation of the process modifications used the equivalent electricity as the parameter of comparison when addressing process modifications for improved process design. The largest reduction of energy consumption in reboiler duty was for the LVC with a flash pressure of 0.5 [bar]. However, it was found in this study that lower flash pressure with more modest reboiler duty reduction, was more attractive since the compression work was considerable higher for the 0.5 [bar] flash.

The equivalent electricity should be calculated as result of local parameters and considering local heat sources and utilization.

It was found that absorption cooling had a large impact on the system. By cooling the fluids in the absorption column, the kinetic conditions could be driven to higher loadings, hence reduced solvent flow rates. Final optimization of the cooling was not attempted in this study. The trends however, imply a large potential for improvement by introducing more and correct cooling, such as several cooling stages. Lean vapor compression gave the largest reduction in reboiler duty, with a 33.4% reduction. The intercooled absorber with the least solvent flow rate gave the largest reduction in equivalent electricity, with a 19.5% reduction, and a solvent flow rate reduction of 63.6%. The rich solvent split modification gave the second largest reduction in equivalent electricity, with a 16% reduction, and no reduction in solvent flow rate.

The reduction in energy specific energy requirement was found to be in good agreement with other sources found in the literature for 30[wt%] AMP, hence suggesting that the values are reasonable. The specific energy reduction for the process modifications, also agreed well with numbers found in literature.

In regards to the application of AMP for biogas upgrading, this thesis suggest that comprehensive cooling is needed in the absorption column in order to have reasonable solvent flow rates in the system. It was assumed that the higher heat of reaction, drove the temperature increase to levels eventually limiting the absorption in the column. The findings of this thesis suggest that AMP has a significant potential for application in biogas upgrading plants, and an interesting candidate for further studies. In comparison with biogas upgrading systems using other processes such as water scrubbing, it is important to reduce operational costs, seen for 250 and 500 [m^3/h] in Table 3.1. Implementing process modifications can lead to reduced energy requirements for the process, and may prove to be an effective method for reducing the operational cost.

.

8.1 Further Work

Based on the simulations in this study, an interesting next step would be to further refine simulations and to test, with possible process modifications, the model in a pilot plant. The purpose of the pilot study would be twofold. Firstly to evaluate AMP for biogas upgrading in plant scale operations. Secondly to evaluate and compare the plant improvements of the process modifications to the simulated values in this thesis, when 30[wt%] AMP is applied. This could provide a good starting point for optimization of other CO_2 absorption plants when AMP

is applied, and for application of AMP in biogas upgrading plants as a possible alternative to MDEA.

In regards to the process modifications addressed in this thesis, further studies should be conducted on intercooling optimization, in order to identify optimal flow rate, cooling temperature, split fraction and cooling stage. In such a study, several intercooling stages should also be addressed. Further on, an interesting next step based on this thesis would be to combine two or more modifications, to identify the interaction between modifications and to possibly reduce the energy consumption further.

Cost estimation has not been included in the scope of this project. This should be conducted in order to evaluate the feasibility of the system(s), hereunder application of process modifications and biogas upgrading with AMP.

Bibliography

[1] J. R. Petit, J. Jouzel, D. Raynaud, N. I. Barkov, J. M. Barnola, I. Basile, M. Bender, J. Chappellaz, M. Davis, G. Delaygue, M. Delmotte, V. M. Kotlyakov, M. Legrand, V. Y. Lipenkov, C. Lorius, L. PÃl'pin, C. Ritz, E. Saltzman, and M. Stievenard, "Climate and atmospheric history of the past 420,000 years from the vostok ice core, antarctica," *Nature*, vol. 399, no. 6735, p. 429, 1999.

[2] D. R. Keeling and D. P. Tans, "The keeling curve," 2016.

[3] BP, "Bp energy outlook," report, 2016.

[4] International Energy Agency, "World energy outlook 2015," report, 2015.

[5] O. Edenhofer, R. Pichs-Madruga, Y. Sokona, E. Farahani, S. Kadner, K. Seyboth, A. Adler, I. Baum, S. Brunner, P. Eickemeier, B. Kriemann, J. Savolainen, S. Schlömer, C. von Stechow, T. Zwickel, and J. Minx, "Climate change 2014: Mitigation of climate change," report, IPCC, 2014.

[6] United States Environmental Protection Agency, "Carbon dioxide capture and sequestration." `https://www3.epa.gov/climatechange/ccs/`, 2016. Accessed 19.06.2016.

[7] F. Bauer, C. Hultenberg, P. Tobias, and D. Tamm, "Biogas upgrading - review of commercial technologies," report, Svenskt gastekniskt center AB, 2013.

[8] IEA Bioenergy Task 37, "Country reports summary 2015," report, 2016.

[9] Skog Norske, "Biokraft." `http://www.biokraft.no/biokraft-skogn/`, 2016. Accessed 02.06.2016.

[10] Greve Biogass, "Greve biogass." http://www.grevebiogass.no/greve-biogass/, 2016. Accessed 03.06.2016.

[11] Romerike Biogassanlegg, "Romerike biogassanlegg." https://www.oslo.kommune.no/avfall-og-gjenvinning/behandlingsanlegg-for-avfall/romerike-biogassanlegg/, 2016. Accessed 03.06.2016.

[12] Innovasjon Norge, "20 millioner til pilotprosjekt for biogass." http://www.innovasjonnorge.no/no/Nyheter/20-millioner-til-pilotprosjekt-for-biogass/#.V1FCNpF95hG, 2016. Accessed 03.06.2016.

[13] R. Bottoms, "Process for separating acidic gases," 1930.

[14] U. E. Aronu, H. F. Svendsen, K. A. Hoff, and O. Juliussen, "Solvent selection for carbon dioxide absorption," *Energy Procedia*, vol. 1, no. 1, pp. 1051–1057, 2009.

[15] K. Goto, H. Okabe, S. Shimizu, M. Onoda, and Y. Fujioka, "Evaluation method of novel absorbents for co2 capture," *Energy Procedia*, vol. 1, no. 1, pp. 1083–1089, 2009.

[16] F. A. Tobiesen, O. Juliussen, and H. F. Svendsen, "Experimental validation of a rigorous desorber model for post-combustion capture," *Chemical Engineering Science*, vol. 63, no. 10, pp. 2641–2656, 2008.

[17] G. Sartori and D. W. Savage, "Sterically hindered amines for carbon dioxide removal from gases," *Industrial and Engineering Chemistry Fundamentals*, vol. 22, no. 2, pp. 239–249, 1983.

[18] D. J. Seo and W. H. Hong, "Solubilities of carbon dioxide in aqueous mixtures of diethanolamine and 2-amino-2-methyl-1-propanol," *Journal of Chemical and Engineering Data*, vol. 41, no. 2, pp. 258–260, 1996.

[19] M. Kundu, B. P. Mandal, and S. S. Bandyopadhyay, "Vapor-liquid equilibrium of co 2 in aqueous solutions of 2-amino-2-methyl-1-propanol," 2003.

[20] H. Svensson, J. Edfeldt, V. Zejnullahu Velasco, C. Hulteberg, and H. T. Karlsson, "Solubility of carbon dioxide in mixtures of 2-amino-2-methyl-1-propanol and organic solvents," *International Journal of Greenhouse Gas Control*, vol. 27, pp. 247–254, 2014.

[21] A. K. Chakraborty, G. Astarita, and K. B. Bischoff, "Co2 absorption in aqueous solutions of hindered amines," *Chemical Engineering Science*, vol. 41, no. 4, pp. 997–1003, 1986.

[22] G. D. Pappa, C. Anastasi, and E. C. Voutsas, "Measurement and thermodynamic modeling of the phase equilibrium of aqueous 2-amino-2-methyl-1-propanol solutions," *Fluid Phase Equilibria*, vol. 243, no. 1âĂŞ2, pp. 193–197, 2006.

[23] T. Neveux, Y. Le Moullec, J. P. Corriou, and F. Eric, "Energy performance of co2 capture processes: Interaction between process design and solvent," *CHEMICAL ENGINEERING TRANSACTIONS*, vol. 35, 2013.

[24] A. Hartono, M. Saeed, A. F. Ciftja, and H. F. Svendsen, "Binary and ternary vle of the 2-amino-2-methyl-1-propanol (amp)/piperazine (pz)/water system," *Chemical Engineering Science*, vol. 91, pp. 151–161, 2013.

[25] I. Kim, H. Svendsen, and E. Borresen, "Ebulliometric determination of vapor-liquid equilibria for pure water, monoethanolamine, n-methyldiethanolamine, 3-(methylamino)-propylamine, and their binary and ternary solutions," *J. Chem. Eng. Data*, vol. 53, no. 11, pp. 2521–2531, 2008.

[26] I. Kim and H. F. Svendsen, "Comparative study of the heats of absorption of post-combustion co2 absorbents," *International Journal of Greenhouse Gas Control*, vol. 5, no. 3, pp. 390–395, 2011.

[27] A. Cousins, L. T. Wardhaugh, and P. H. M. Feron, "Preliminary analysis of process flow sheet modifications for energy efficient co2 capture from flue gases using chemical absorption," *Chemical Engineering Research and Design*, vol. 89, no. 8, pp. 1237–1251, 2011.

[28] A. Cousins, L. T. Wardhaugh, and P. H. M. Feron, "A survey of process flow sheet modifications for energy efficient co2 capture from flue gases using chemical absorption," *International Journal of Greenhouse Gas Control*, vol. 5, no. 4, pp. 605–619, 2011.

[29] H. Ahn, M. Luberti, Z. Liu, and S. Brandani, "Process configuration studies of the amine capture process for coal-fired power plants," *International Journal of Greenhouse Gas Control*, vol. 16, pp. 29–40, 2013.

[30] Y. Le Moullec and M. Kanniche, "Screening of flowsheet modifications for an efficient monoethanolamine (mea) based post-combustion co 2 capture," *International Journal of Greenhouse Gas Control*, vol. 5, no. 4, pp. 727–740, 2011.

[31] B. A. Oyenekan and G. T. Rochelle, "Alternative stripper configurations for co2 capture by aqueous amines," *AIChE Journal*, vol. 53, no. 12, 2007.

[32] Y. Le Moullec, T. Neveux, A. Al Azki, A. Chikukwa, and K. A. Hoff, "Process modifications for solvent-based post-combustion co2 capture," *International Journal of Greenhouse Gas Control*, vol. 31, pp. 96–112, 2014.

[33] M. Karimi, M. Hillestad, and H. F. Svendsen, "Capital costs and energy considerations of different alternative stripper configurations for post combustion co2 capture," *Chemical Engineering Research and Design*, vol. 89, no. 8, pp. 1229–1236, 2011.

[34] M. Karimi, M. Hillestad, and H. F. Svendsen, "Investigation of intercooling effect in co2 capture energy consumption," *Energy Procedia*, vol. 4, pp. 1601–1607, 2011.

[35] J. N. Knudsen, J. Andersen, J. N. Jensen, and O. Biede, "Evaluation of process upgrades and novel solvents for the post combustion co2 capture process in pilot-scale," *Energy Procedia*, vol. 4, pp. 1558–1565, 2011.

[36] B. Baburao and C. Schubert, "Advanced intercooling and recycling in co2 absorption," 2014.

[37] R. F. Strigle and R. F. Strigle, *Packed tower design and applications : random and structured packings*. Houston: Gulf Publ. Co., 2nd ed. ed., 1994. Strigle, Ralph F.

[38] T. Dixon, H. Herzog, S. Twinning, J. Gervasi, L. Dubois, and D. Thomas, "12th international conference on greenhouse gas control technologies, ghgt-12simulation of the post-combustion co2 capture with aspen hysystm software: Study of different configurations of an absorption-regeneration process for the application to cement flue gases," *Energy Procedia*, vol. 63, pp. 1018–1028, 2014.

[39] J. Naumovitz and M. Koch, "Method and system for reducing energy requirements of a co2 capture system," 2012.

[40] J. Gabrielsen, *CO 2 Capture from Coal Fired Power Plants*. Thesis, 2007.

[41] J. Gabrielsen, H. F. Svendsen, M. L. Michelsen, E. H. Stenby, and G. M. Kontogeorgis, "Experimental validation of a rate-based model for co 2 capture using an amp solution," *Chemical Engineering Science*, vol. 62, no. 9, pp. 2397–2413, 2007.

[42] F. A. Tobiesen, H. F. Svendsen, and O. Juliussen, "Experimental validation of a rigorous absorber model for co 2 postcombustion capture," *AIChE Journal*, vol. 53, no. 4, pp. 846–865, 2007.

[43] P. Tontiwachwuthikul, A. Meisen, and C. J. Lim, "Co2 absorption by naoh, monoethanolamine and 2-amino-2-methyl-1-propanol solutions in a packed column," *Chemical Engineering Science*, vol. 47, no. 2, pp. 381–390, 1992.

[44] A. Aroonwilas and P. Tontiwachwuthikul, "High-efficiency structured packing for co2 separation using 2-amino-2-methyl-1-propanol (amp)," *Separation and Purification Technology*, vol. 12, no. 1, pp. 67–79, 1997.

[45] S. K. Dash, A. N. Samanta, and S. S. Bandyopadhyay, "(vapour + liquid) equilibria (vle) of co 2 in aqueous solutions of 2-amino-2-methyl-1-propanol: New data and modelling using enrtl-equation," *The Journal of Chemical Thermodynamics*, vol. 43, no. 8, pp. 1278–1285, 2011.

[46] M. H. Li and B. C. Chang, "Solubilities of carbon dioxide in water + monoethanolamine + 2-amino-2-methyl-1-propanol," *Journal of Chemical and Engineering Data*, vol. 39, no. 3, 1994.

[47] D. Silkenbaeumer and R. N. Lichtenthaler, "Solubility of carbon dioxide in aqueous solutions of 2-amino-2-methyl-1-propanol and n-methyldiethanolamine and their mixtures in the temperature range of 313 to 353 k and pressures up to 2.7 mpa," *Industrial and Engineering Chemistry Research*, vol. 37, no. 8, pp. 3133–3141, 1998.

[48] T. T. Teng and A. E. Mather, "Solubility of co 2 in an amp solution," *Journal of Chemical and Engineering Data*, vol. 35, no. 4, pp. 410–411, 1990.

[49] D. Tong, J. Trusler, G. Maitland, J. Gibbins, P. Fennell, and D. Tong, "Solubility of carbon dioxide in aqueous solution of monoethanolamine or 2-amino-2-methyl-1-propanol: Experimental measurements and modelling," *International Journal of Greenhouse Gas Control*, vol. 6, pp. 37–47, 2012.

[50] P. Tontiwachwuthikul, A. Meisen, and C. J. Lim, "Solubility of co2 in 2-amino-2-methyl-1-propanol solutions," *J. Chem. Eng. Data*, vol. 36, no. 1, pp. 130–133, 1991.

[51] M. Beil, W. Beyrich, U. Holzhammer, and T. Krause, "Biomethane," report, 2013.

[52] A. Akbulut, "Techno-economic analysis of electricity and heat generation from farm-scale biogas plant: Cicekdagi case study," *Energy*, vol. 44, no. 1, pp. 381–390, 2012.

[53] L. Hinge and J. Hinge tech. rep.

[54] G. P. Towler and R. K. Sinnott, *Chemical engineering design*. Chemical Engineering Design - SI Edition, Oxford: Butterworth-Heinemann, 5th ed. / by gavin towler, ray sinnott. ed., 2009.

[55] A. Technology, "Aspen plus user guide," 2000.

[56] R. Billet and M. Schultes, "Prediction of mass transfer columns with dumped and arranged packings: Updated summary of the calculation method of billet and schultes," *Chemical Engineering Research and Design*, vol. 77, no. 6, pp. 498–504, 1999.

[57] J. L. Bravo, J. A. Rocha, and J. R. Fair, "Mass transfer in guaze packings," *Hydrocarbon Processing*, vol. 64, no. 91, 1985.

[58] T. Mejdell, T. Vassbotn, O. Juliussen, A. Tobiesen, A. Einbu, H. Knuutila, K. A. Hoff, V. Andersson, and H. F. Svendsen, "Novel full height pilot plant for solvent development and model validation," *Energy Procedia*, vol. 4, pp. 1753–1760, 2011.

[59] S. L. Simone Gamba, Laura A. Pellegrini*, "Energy analysis of different municipal sewage sludge- derived biogas upgrading techniques," *Chemical Engineering Transactions*, vol. 37, 2014.

[60] A. Krotki, L. Wieclaw-Solny, A. Tatarczuk, M. Stec, A. Wilk, D. Spiewak, and T. Spietz, "Laboratory studies of post-combustion co2 capture by absorption with mea and amp solvents," *Arab. J. Sci. Eng.*, vol. 41, no. 2, pp. 371–379, 2016.

[61] P. Singh, W. P. M. Van Swaaij, and D. W. F. Brilman, "Energy efficient solvents for co2 absorption from flue gas: Vapor liquid equilibrium and pilot plant study," *Energy Procedia*, vol. 37, pp. 2021–2046, 2013. (Wim).

[62] J. Gale, C. Hendriks, W. Turkenberg, H. M. Kvamsdal, G. Haugen, H. F. Svendsen, A. Tobiesen, H. Mangalapally, A. Hartono, and T. Mejdell, "10th international conference on greenhouse gas control technologiesmodelling and simulation of the esbjerg pilot plant using the cesar 1 solvent," *Energy Procedia*, vol. 4, pp. 1644–1651, 2011.

Appendices

Appendix A

Vapor Liquid Equilibria Simulations

The vapor-liquidequilibrium simulation results are shown here. It can be seen that the model and experimental data is more accurate for lower loadings and temperatures. Graphical representation of VLE simulations of AMP concentrations other than 3.4M are not given in this report, as these are not used in further work.

Table A.1: Absolute average deviation show for the various experimental sources evaluated against simulation data.

Ref.	**C[mol/L]**	**T[K]**	α **[molCO$_2$/molAMP]**		**AAD[%]**
			High	**Low**	
Dash et al.	2.5	298	1.100	0.461	15.8
	2.5	308	1.073	0.313	17.9
	2.5	318	1.074	0.274	21.6
	2.5	328	1.045	0.232	24.7
	3.4	298	1.056	0.426	59.3
	3.4	308	1.040	0.301	32.3
	3.4	318	1.050	0.282	39.0
	3.4	328	1.009	0.291	32.6
	4.9	298	1.032	0.337	1332.5
	4.9	308	1.015	0.260	882.2
	4.9	318	1.001	0.216	680.2
	4.9	328	0.962	0.191	456.0
Li and Chang	3.3	313	0.867	0.396	37.6
	3.3	333	0.721	0.200	13.6
	3.3	353	0.617	0.102	12.6
	3.3	373	0.343	0.039	35.4
Seo and Hong	3.3	313	0.899	0.500	33.5
	3.3	333	0.843	0.342	10.3
	3.3	353	0.711	0.279	29.5
Tong and Trusler	3.4	313	0.965	0.683	46.1
	3.4	333	0.924	0.618	53.1
	3.4	353	0.778	0.438	45.5
	3.4	373	0.782	0.045	31.6
	3.4	393	0.429	0.048	11.1
Tontiwachwuthikul et. Al	2.0	293	0.960	0.781	27.2
	2.0	313	0.940	0.620	29.7
	2.0	333	0.830	0.375	41.1
	2.0	353	0.618	0.154	44.2
	3.0	293	0.898	0.747	65.2
	3.0	313	0.875	0.582	43.3
	3.0	333	0.809	0.321	38.9
	3.0	353	0.524	0.126	27.9
Teng and Mather	2.0	313	1.001	0.035	43.5
	2.0	343	1.265	0.033	41.8
Kundu et al.	2.0	303	0.966	0.674	5.3
	2.8	303	0.938	0.689	13.6
	2.8	313	0.924	0.527	18.3
	2.8	323	0.841	0.430	7.0
	3.4	303	0.889	0.599	10.6
	3.4	313	0.876	0.475	27.0
	3.4	323	0.781	0.412	14.0

Appendix B

Deviation Calulation

The equations used for calculated deviation is stated in this appendix. The average deviation is calculated according to Equation B.1.

$$x_i = \frac{\nu_{sim} - \nu_{exp}}{\nu_{exp}} \times 100 \tag{B.1}$$

where ν_{sim} and ν_{exp} are the compared values from simulation and experimental data respectively. The percentage deviation was used to calculate the average deviation(AD) and the absolute deviation (AAD), calculated by the following formulas:

$$AD = \frac{1}{n} \sum_{n}^{i=1} |x_i| \tag{B.2}$$

$$AAD = \frac{1}{n} \sum_{n}^{i=1} |x_i - \bar{x}_i| \tag{B.3}$$

$$\bar{x} = \frac{\sum_{n}^{i=1} x_i}{n} \tag{B.4}$$

Appendix C

Absorption Results

The specified experimental data from the absorption pilot plant study by [41] and the simulated data for the pilot are shown in this appendix.

Table C.1: Comparison of simulation and experimental results

Run#	Solv	T[°C]		CO_2Inlet	Lean	Nco2		Nabs		Nabs	%dev	|%dev-$\bar{x}$|
		Lean	Flue	gas	loading	Lin	Lout	Exp	Sim	(sim/exp)		
	(l/min)	solv	Gas	(vol%)	(α)	(kmol/h)				[-]		
1	3	40	40	2.62	0.072	0.037	0.091	0.054	0.065	1.199	19.95	20.27
2	6	41	41	2.38	0.095	0.097	0.155	0.058	0.067	1.165	16.47	16.79
3	6	41	39	4.82	0.084	0.086	0.174	0.088	0.110	1.248	24.81	25.13
4	3	40	41	9.28	0.118	0.061	0.198	0.137	0.129	0.945	-5.52	5.20
5	3	41	40	4.81	0.142	0.073	0.147	0.074	0.075	1.020	1.98	2.31
6	6	41	41	4.41	0.147	0.153	0.236	0.083	0.086	1.039	3.87	4.20
7	3	41	41	12.96	0.170	0.088	0.239	0.151	0.135	0.892	-10.84	10.52
8	6	40	39	5.33	0.219	0.227	0.341	0.114	0.105	0.923	-7.70	7.37
9	3	40	40	4.90	0.309	0.161	0.208	0.047	0.032	0.672	-32.85	32.52
10	3	40	39	11.33	0.272	0.142	0.249	0.107	0.091	0.851	-14.91	14.58
11	6	40	39	10.27	0.284	0.295	0.417	0.122	0.123	1.012	1.16	1.48

Appendix D

Desorption Results

The specified experimental data from the desorption pilot plant study by [41] and the simulated data for the pilot are shown in this appendix. Table D.2 gives the first simulation effort of the desorption column. Table D.1 shows the second simulation effort, which gave improved temperature profiles in the desorption column.

Table D.1: Comparison of second and altered simulation and experimental results for the desorption column. The AAD and AD was calculated as 8.0% and 14.1% respectively.

Run #	Solvent flow (l/min)	Reboiler duty [kW]	Temp rich solv [°C]	Rich Solv loading [α]	CO_2 from stripper kg/h	NdesCO$_2$ exp kmol/h	NdesCO$_2$ sim kmol/h	Ndes (sim/exp)	%dev	|%dev|	|%dev-$\bar{x}$|
1	3	5.8	111	0.178	2.69	0.061	0.055	0.902	-9.78	9.78	4.34
2	6	7.6	114	0.151	2.66	0.060	0.061	1.001	0.10	0.10	14.21
3	6	9.4	114	0.169	4.19	0.095	0.087	0.909	-9.07	9.07	5.05
4	3	7.6	104	0.379	6.9	0.157	0.124	0.790	-21.01	21.01	6.90
5	3	5.8	107	0.282	3.51	0.080	0.074	0.929	-7.12	7.12	7.00
6	6	7.6	110	0.226	3.8	0.086	0.080	0.922	-7.84	7.84	6.28
7	3	7.6	99	0.459	7	0.159	0.133	0.837	-16.30	16.30	2.19
8	6	7.7	107	0.327	6	0.136	0.103	0.759	-24.09	24.09	9.98
9	3	3.9	97	0.398	2.05	0.047	0.043	0.929	-7.10	7.10	7.02
10	3	5.8	98	0.479	6	0.136	0.096	0.704	-29.56	29.56	15.45
11	6	7.7	103	0.4	6.48	0.147	0.113	0.765	-23.49	23.49	9.37

Table D.2: Comparison of simulation and experimental results for the all equilibrium reactions desorption column. The AAD and AD was calculated as 7.1% and 17.0% respectively.

Run #	Solvent flow (l/min)	Reboiler duty [kW]	Temp rich solv [C]	Rich Solv loading [a]	CO2 from stripper kg/h	NdesCO2 exp kmol/h	NdesCO2 sim kmol/h	Ndes (sim/exp)	%dev	|%dev|	|%dev-x|
1	3	5.8	111	0.178	2.69	0.061	0.052	0.857	-14.32	14.32	0.21
2	6	7.6	114	0.151	2.66	0.060	0.058	0.967	-3.28	3.28	10.83
3	6	9.4	114	0.169	4.19	0.095	0.083	0.873	-12.65	12.65	1.46
4	3	7.6	104	0.379	6.90	0.157	0.119	0.758	-24.20	24.20	10.08
5	3	5.8	107	0.282	3.51	0.080	0.071	0.892	-10.83	10.83	3.28
6	6	7.6	110	0.226	3.80	0.086	0.077	0.890	-11.05	11.05	3.07
7	3	7.6	99	0.459	7.00	0.159	0.129	0.811	-18.85	18.85	4.74
8	6	7.7	107	0.327	6.00	0.136	0.101	0.739	-26.11	26.11	12.00
9	3	3.9	97	0.398	2.05	0.047	0.042	0.909	-9.12	9.12	4.99
10	3	5.8	98	0.479	6.00	0.136	0.094	0.690	-31.02	31.02	16.91
11	6	7.7	103	0.400	6.48	0.147	0.110	0.749	-25.09	25.09	10.98

Appendix E

Optimal Flow Rates

The L/G vs duty diagrams are given in this appendix. These analysis's were performed to find the optimal operation in regards to reduced reboiler duty and solvent flow rate.

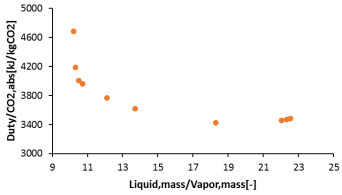

(a) Base case

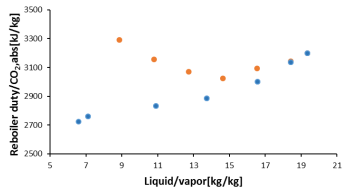

(b) ICA

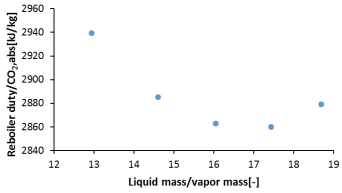

(c) FGC

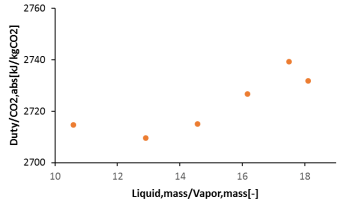

(d) LVC

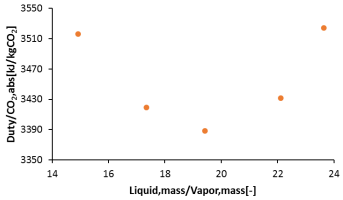

(e) RVC

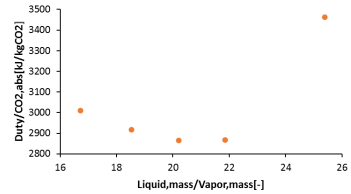

(f) RSS

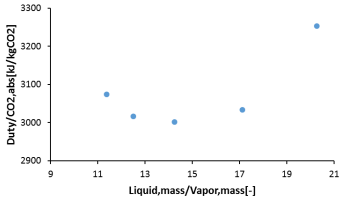

(g) RSR

Figure E.1: Optimized liquid to gas mass flow rate in the absorption column for the different modifications.